JACS
JOURNAL OF THE AMERICAN CHEMICAL SOCIETY

ARTICLE

pubs.acs.org/JACS

Organoactinides Promote the Dimerization of Aldehydes: Scope, Kinetics, Thermodynamics, and Calculation Studies

Manab Sharma,[†,‡] Tamer Andrea,[†] Nigel J. Brookes,[‡] Brian F. Yates,[‡] and Moris S. Eisen*[,†]

[†]Schulich Faculty of Chemistry, Institute of Catalysis Science and Technology, Technion—Israel Institute of Technology, Technion City, 32000 Haifa, Israel

[‡]School of Chemistry, University of Tasmania, Hobart, Tasmania, Australia

Supporting Information

ABSTRACT: Surprising catalytic activities have been found for the actinide complexes $Cp^*_2ThMe_2$ (**1**), $Th(NEtMe)_4$ (**2**), and $Me_2SiCp''_2Th(C_4H_9)_2$(**3**) toward oxygenated substrates. During the catalytic dimerization of benzaldehydes to their corresponding esters, complexes **1** and **2** gave 65 and 85% yield in 48 h, respectively, while the geometry-constrained complex **3** gave 96% yield in 24 h. Exploring the effect of substituents on benzaldehyde, it has been found that, in general, electron-withdrawing groups facilitate the reaction. Kinetic study with complexes **1** and **3** reveals that the rate of the reaction is first order in catalyst and substrate, which suggests the rate equation "rate = k[catalyst]^1-[aldehyde]^1". The activation energy of the reaction was found to be 7.16 ± 0.40 and 3.47 ± 0.40 kcal/mol for complexes **1** and **3** respectively, which clearly indicates the advantage of the geometry-constrained complex. Astonishing are the reactivity of the organoactinide complexes with oxygen-containing substrates, and especially the reactivity of complex **3**, toward the dimerization of substrates like *p*-methoxybenzaldehyde, *m*/*p*-nitrobenzaldehyde, and furanaldehyde and the reactivity toward the polymerization of terephthalaldehyde. Density functional theory mechanistic study reveals that the catalytic cycle proceeds via an initially four-centered transition state (+6 kcal/mol), followed by the rate-determining six-centered transition state (+13.5 kcal/mol), to yield thermodynamically stable products.

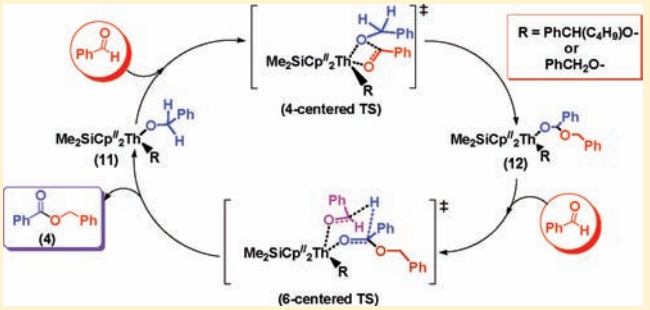

INTRODUCTION

The catalytic dimerization of aldehydes to give the corresponding esters (known as the Tishchenko reaction) is a century-old process. Due to its atom efficiency, the reaction is still drawing worldwide attention among industrial and academic researchers.[1] Since its first discovery in 1887, and a further modification in 1906,[2] aluminum alkoxides have been the traditional homogeneous catalysts to perform this reaction.[3] During the past decade, in addition to aluminum complexes, many other catalysts have been screened, e.g., boron,[4] iron,[5] zirconium,[6] ruthenium,[7] rhodium,[8] lanthanum,[9] neodymium,[9a] ytterbium,[9b] hafnium,[6] osmium,[10] and iridium,[11] but interestingly, never actinides. It is essential to indicate that, when aromatic aldehydes are used, the majority of the catalysts show a sluggish activity for the coupling reaction.

The lanthanide complexes $Cp^*_2LnCH(SiMe_3)_2$ (Ln = La, Nd; $Cp^* = C_5Me_5$) were found to catalyze the Tishchenko reaction of aromatic aldehydes in moderate yields,[9a,9b] but the reaction usually required heating for 3 days at 60 °C. The corresponding homoleptic lanthanides $Ln[N(SiMe_3)_2]_3$ (Ln = La, Y, Sm)[9b,9d] were found to be more reactive, with higher turnover frequencies, when electron-withdrawing ligands were used. Group 4 complexes, such as $Cp^*_2MH_2$ and $Cp^*_2M(Cl)H$ (M = Zr, Hf),[6] were found to be highly efficient in the dimerization of aliphatic aldehydes but inactive toward aromatic aldehydes. Moreover, homologous titanocene complexes were found to be inert under all conditions.[6]

In contrast to the rich chemistry that has been offered by organolanthanide complexes during the past two decades, the electrophilic d^0/f^n chemistry of organoactinide compounds has been under a fervent investigation and has achieved a high level of sophistication due to the unique structure—reactivity relationships of the organoactinides[12] and their outstanding performance in various homogeneous catalytic processes.[13] For example, catalytic reactions involving neutral organoactinides were first limited to C—H activations and hydrogenation of hydrocarbons.[13] However, recent applications of organoactinide complexes in challenging catalytic organic chemical transformations like hydroamination,[13n,o] oligomerization,[13g,13h] selective dimerization,[14] hydrosilylation of alkene and alkynes,[15] coupling of silanes with amines,[13t] coupling of isonitriles with alkynes,[16] disproportionation metathesis of TMSC≡CH, and cross-metathesis of TMSC≡CH or

Received: June 28, 2010
Published: January 11, 2011

TMSC≡CTMS with various terminal alkynes[12m,17] have taken this chemistry to a new level.

The stoichiometric and catalytic properties of organo-f-element complexes are deeply influenced by the nature of the π ancillary ligands.[12g,12i,12p,12t,18] The justification for the commonly used pentamethylcyclopentadienyl ligand relates to the fact that it allows researchers to obtain simple organoactinide complexes with good solubility, thermal stability, and resistance to ligand redistribution.[19] Structurally, a significant opening of the metal coordination sphere (frontier orbitals)[20] at the σ-ligand equatorial girdle is obtained by replacing the pentamethylcyclopentadienyl ligation in $Cp^*_2MR_2$ (M = f-element metal, R = σ-bonded ligand) by a bridged ligand such as *ansa*-$Me_2SiCp''_2MR_2$ ($Cp'' = C_5Me_4$).[13a,21] For organolanthanides, this alteration allowed an increase of 10−100-fold in rates for the olefin insertion into a M−R bond,[22] whereas in organoactinides, this modification has been shown to cause an increase of 10^3-fold in their catalytic activity in the hydrogenation of 1-hexene and in the hydrosilylation of alkynes and alkenes.[21c,22a]

In spite of the successful application of organoactinide complexes toward various catalytic transformations, all oxygenated substrates have been excluded on account of the high oxophilicity of the organoactinides, which is expected to lower the activity due to the predictably strong oxygen−actinide interactions. For instance, it has been shown that the use of an alkoxy ligand in place of an alkyl ligand resulted in a reduced catalytic activity in the organoactinide-catalyzed hydrogenation of olefins.[23] Despite those findings, we have recently disclosed a new strategy for the introduction of organoactinides as outstanding catalysts with surprising activities toward the polymerization of cyclic mono- and diesters.[24a] The strategy was designed with a metal−oxygen bond[24b−24e] thermodynamically reacting/inserting with a substrate to form a second metal−oxygen bond, with similar bond energies, with entropy being the main parameter governing the reaction (eqs 1 and 2).

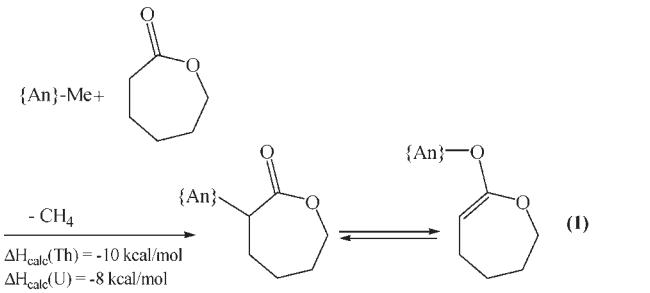

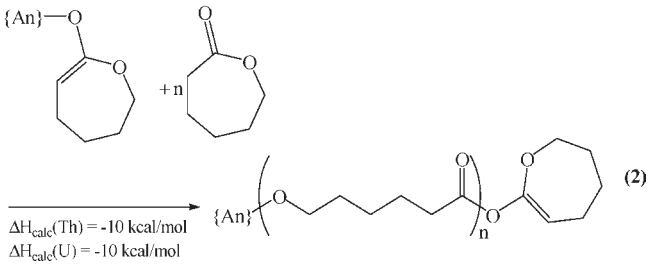

In view of this, we were intrigued by the reactivity of oxygen-containing actinide complexes and wished to study the competition between oxophilicity and coordinative unsaturation of *ansa* complexes. Hence, we have synthesized the oxo-bridged organoactinide complex $\{Me_2SiCp''_2U(^nBu)\}_2(\mu\text{-O})$ ($Cp'' = C_5Me_4$) (Figure 1),

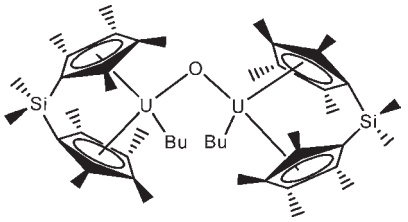

Figure 1. Oxo-bridged uranium complex.

having an *ansa*-type ligand mimicking the model of reactive M−O−M skeletons (M = metal), serving as oxide-supported heterogeneous organometallic catalysts or metal-oxide-containing catalysts.[25] This complex was found to be extremely active for the C−H and C−Si bond activations of aromatic silanes and benzene (eq 3).[17a,26]

$$PhSiH_3 + C_6D_6 \xrightarrow{\{Me_2SiCp''_2U(^nBu)\}_2(\mu\text{-O})} C_6D_5SiH_3 + H_2/HD + Ph_2SiH_2 + SiH_4 \quad (3)$$

On the basis of these results (eqs 1−3), we were interested to study the scope of the insertion of a carbonyl substrate into a metal−oxygen bond (eq 4) and to investigate if we can perform this transformation catalytically.

Hence, we concentrate our research efforts on the reactivity of actinide complexes, particularly for the dimerization of aldehydes, better known as the Tishchenko reaction. The goal of this investigation was to examine the scope, chemoselectivity, ancillary ligand sensitivity, kinetics, and thermodynamics of the Tishchenko reaction catalyzed by the organothorium complexes $(Cp^*)_2ThMe_2$ (**1**), $Th\{N(CH_3)CH_2CH_3\}_4$ (**2**),[27] and the *ansa*-type bridged $Me_2SiCp''_2Th(n\text{-}C_4H_9)$ (**3**),

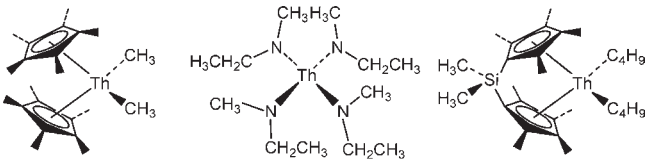

1 **2** **3**

which differ in their ancillary ligation as well as coordinative unsaturation around the metal center, further enabling us to compare the effect of oxophilicity versus their corresponding coordinative unsaturation. Here, we also report the isotope and substituents effects of a variety of aromatic aldehydes on the catalytic reaction. Moreover, computational studies are becoming a vital diagnostic tool to obtain insight into complex reaction mechanisms as well as to reveal various facts about the electronic states or bonding of transition metals,[28] including f-block elements.[29] Therefore, the computational DFT method has been employed to give an explicit account of the reaction mechanism and bonding of various catalytic species and transition-state structures. On the basis of kinetics and thermodynamics together with density functional theory (DFT) studies, a suitable mechanistic pathway is proposed for the studied reaction.

dx.doi.org/10.1021/ja105696p |*J. Am. Chem. Soc.* 2011, 133, 1341–1356

RESULTS

We start by presenting results regarding the different reactivities of the organoactinide complexes with the studied aldehydes. Following this, we disclose the kinetics and thermodynamics studies, including the isotope effect and the effect of substituents, and finally we present some stoichiometric reactions revealing plausible active catalytic species.

Dimerization of Aldehydes by Complexes 1−3. The organoactinide complexes **1**−**3** were found to be active precatalysts for the chemoselective dimerization of aldehydes (eq 5), giving the corresponding esters in high to moderate yields, while no reaction was observed in the absence of a catalyst. Reactions of these complexes were performed with an excess of aldehyde, either in toluene or in benzene (aldehyde:catalyst = 100:1), at room temperature (25 °C), and results for the corresponding ester formation are presented in Table 1. When the same dimerizations were performed at a slightly higher temperature (35 °C), faster reactions were observed (*vide infra*).

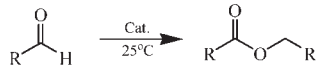

(5)

Cat. = $Cp^*_2ThMe_2$ (**1**); $Th(NEtMe)_4$ (**2**); $Me_2SiCp''_2ThBu_2$ (**3**)

R = Ph, *o*-CH_3Ph, *m*-CH_3Ph, *p*-CH_3Ph, *o*-ClPh, *m*-ClPh, *p*-ClPh, *m*-NO_2Ph, *p*-NO_2Ph, *p*-MeOPh, *p*-CNPh, *p*-(ClIO)Ph, *o*-$(CHO)C_4H_3O$,

The catalytic reactions proceed, in most cases, to completion at the corresponding temperature and were carefully followed by either GC or GC/MS and ^{1}H NMR spectroscopy. All products were isolated and characterized by ^{1}H, ^{13}C, and 2D NMR spectroscopy, GC/MS, high-resolution mass spectroscopy, and when possible by comparison to literature spectra and to data from commercially available analytically pure samples. Isolation protocols for the products involved high-vacuum transfer of volatiles with subsequent elimination of the solvent and final distillation of products or purification by silica gel column chromatography. GC/MS, MALDI-MS, and NMR analysis of the products demonstrated that the esters were the exclusively obtained products.

The reactivity of the complexes with different aromatic aldehydes at various reaction times is presented in Table 1. It has been shown that the coordinative unsaturation of the organoactinide complexes used in this study follows the order **3** > **2** > **1**, suggesting, as can be observed in Table 1, that the higher the coordinative unsaturation of the organoactinide complex, the faster the dimerization (for example, compare entries 1, 8, and 15 or 2, 9, and 16).[13a,20−23] In addition, a large difference in reactivity was observed among the different aldehyde substituents (compare entries 2, 3, and 4 with 5, 6, and 7). For each of the complexes, electron-withdrawing substituents at the aromatic ring induce better reactivities.

Most interesting was the surprising activity of complex **3** toward *p*-nitrobenzaldehyde, *m*-nitrobenzaldehyde, and furfuraldehyde, improving the general scope of the reaction and introducing a new concept regarding the group tolerance of organoactinides. However, in the case of *o*-nitrobenzaldehyde, instead of the desired product, an insoluble material was formed, presumably of a polymeric nature, which we were unable to fully characterize.

The reaction of furfuraldehyde did not proceed at room temperature; however, at 60 °C, 42% yield of the corresponding ester was obtained after 48 h (Table 1, entry 20). To explore further the potential scope of complex **3**, reactions were also carried out with *p*-methoxy- and *p*-cyanobenzaldehyde. The ester product of the reaction with *p*-cyanobenzaldehyde precipitates cleanly out of the solution, and the reaction was found to be reasonably fast, while with *p*-methoxybenzaldehyde the reaction was rather slower (compare entries 15 and 16 in Table 1). The slow conversion of the *p*-methoxybenzaldehyde clearly supports the fact that the presence of an electron-donating group in the phenyl ring decreases the rate of the reaction.

Table 1. Coupling of Aromatic Aldehydes by Complexes 1−3[a]

			yield (%)		
entry	cat.	RCHO	after 6 h	after 24 h	after 48 h
1	**1**	Ph	13	41	65
2	**1**	*p*-CH_3-Ph	3.5	14	25
3	**1**	*m*-CH_3-Ph	2.7	11	20
4	**1**	*o*-CH_3-Ph	1.3	5	10
5	**1**	*p*-Cl-Ph	21	60	84
6	**1**	*m*-Cl-Ph	19	57	81
7	**1**	*o*-Cl-Ph	16	50	75
8	**2**	Ph	21	61	85
9	**2**	*p*-CH_3-Ph	19	58	82
10	**2**	*m*-CH_3-Ph	15	50	75
11	**2**	*o*-CH_3-Ph	9	33	55
12	**2**	*p*-Cl-Ph	37	85	97
13	**2**	*m*-Cl-Ph	33	80	96
14	**2**	*o*-Cl-Ph	32	78	95
15	**3**	Ph	58	96	
16	**3**	*p*-CH_3-Ph	28	74	
17	**3**	*m*-CH_3-Ph	51	94	
18	**3**	*o*-CH_3-Ph	26	70	
12	**3**	*p*-Cl-Ph	75	98	
13	**3**	*m*-Cl-Ph	68	95	
14	**3**	*o*-Cl-Ph	61	89	
15	**3**	*p*-CN-Ph	62	98	
16	**3**	*p*-MeO-Ph	12	39	
17	**3**	*o*-NO_2-Ph	−	−	
18	**3**	*m*-NO_2-Ph	62	98	
19	**3**	*p*-NO_2-Ph	51		
20	**3**	2-furanaldehyde			42[d]
21	**3**	terephthalaldehyde	60[b]		
22	**3**	Ph [c]	49		

[a] Yields were determined from ^{1}H NMR and GC/MS. [b] Conversion. [c] Recycled catalyst. [d] At 60 °C.

It is important to point out that the activity of complex **3** was also screened toward nonaromatic aldehydes, like cyclohexanaldehyde, pivaldehyde, pentanaldehyde, and acetaldehyde, showing for all the reactions only the stoichiometric insertion of two aldehyde molecules into the two Th−C butyl bonds, producing the expected corresponding alkoxides (along with some unidentified products).

Apart from these monoaldehydes, complex **3** was found also to be very active toward a dialdehyde, viz. terephthalaldehyde, forming dimeric as well as oligomeric and polymeric esters (eq 6). During a reaction period of 6 h, at room temperature, a light yellow polymer was formed, which starts precipitating out of the reaction solution. After 20 h, the precipitate was collected by filtration, washed with toluene, dried, and characterized by ^{1}H NMR spectroscopy. Two aldehyde signals, at δ 9.92 and 9.95 ppm, in addition to two sets of

dx.doi.org/10.1021/ja105696p | *J. Am. Chem. Soc.* 2011, 133, 1341–1356

methylene signals, in the ranges δ 4.63−4.71 and 5.24−5.37 ppm, clearly support the presence of two unsymmetrical end aldehydic groups and two different types of methylene groups (*m* and *n* type, eq 6) in the chain. The integration ratio between the aldehyde and methylene signals allows us to calculate the degree of polymerization and the number-average molecular weight (DP = 25; M_n = 3350 g/mol). Analysis of the soluble part of the reaction mixture, even after 20 h, exhibits small amounts (<5%) of oligomers (up to pentamers as exhibited by MALDI-TOF).

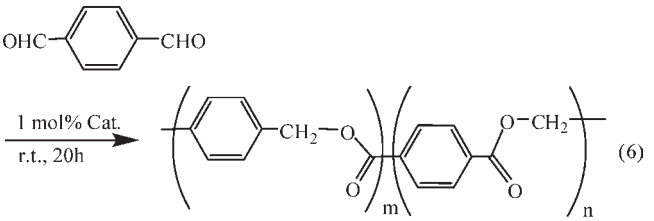

Cat. = $Me_2SiCp''_2ThBu_2$ (**3**)

One of the most important queries regarding catalytic processes is the fate of the catalysts after a batch of reaction. Regarding complex **3**, we were astonished to find that, on completion of one batch of the polymerization reaction (eq 6), when the solution was charged again with the same amount of terephthalaldehyde, precipitation of the polymer was again observed, producing almost the same results as obtained after 6 h of the first batch of reaction. In addition, during a typical recycling experiment with complex **3** for the dimerization of benzaldehyde (eq 5), 85% of the initial activity was found to be retained by the catalyst, which further supports the longer durability as well as stability of the complex (Table 1, entry 22).

The conceptual cross-coupling Tishchenko reaction between two different aldehydes (benzaldehyde and *p*-tolualdehyde) to afford four possible esters (eq 7) was also studied using complex **1**, and the results are presented in Table 2. As expected, the relative reactivity of the corresponding aldehydes is the main factor toward a chemoselective product. As benzaldehyde is more active than *p*-tolualdehyde, product **4** is expected to be obtained in higher yields. It must be taken into account that, since there are few kinetic steps (*vide infra*), the reaction can be tailored by changing the ratio of the two substrates. A simple illustration was made by using 1:1, 1:2, and 2:1 benzaldehyde:*p*-tolualdehyde ratios (Table 2).

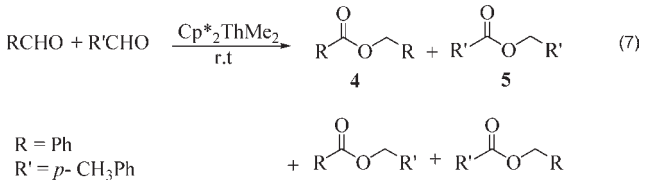

Kinetic and Thermodynamic Studies of the Tishchenko Reaction of Benzaldehyde Promoted by Complexes 1 and 3. In order to propose a plausible mechanism for the reaction, to gain a better understanding of the effect of the ancillary ligands, and to learn about the influence of the aldehyde and the catalyst on the reaction rate, kinetics measurements were performed. The catalytic reaction of 2 aldehyde → ester promoted by $Cp^*_2ThMe_2$ and $Me_2SiCp''_2Th^nBu_2$ was followed by *in situ* ^{1}H NMR spectroscopy in benzene-d_6 or toluene-d_8. The progress of the reaction was monitored by the disappearance of the terminal aldehyde hydrogen, C(O)*H* (δ = 9.60 ppm), along with the appearance the proton

Table 2. Cross-Tishchenko Reaction of Benzaldehyde and *p*-Tolualdehyde Catalyzed by Complex 1[a]

		yield (%)			
entry	cat.:RCHO:R′CHO	**4**	**5**	**6**	**7**
1	1:100:100	15	4	6	6
2	1:100:50	25	2	5	5
3	1:50:100	9	6	6	6

[a] 24 h. Yields were determined from the integration of ^{1}H NMR spectra and GC/MS.

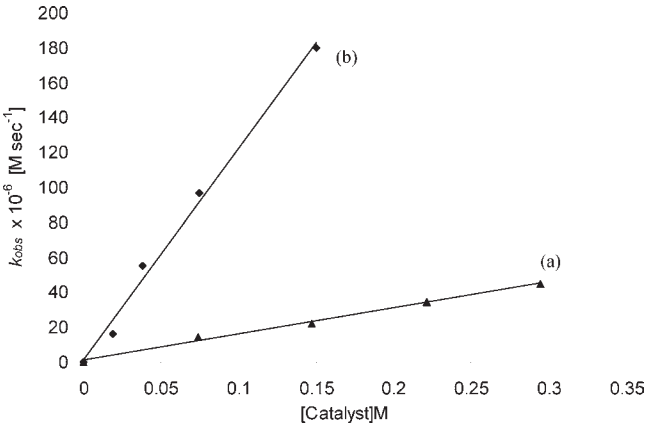

Figure 2. Variation of reaction rate (k_{obs}) with concentration of precatalysts (a) **1** and (b) **3**.

α to the carbonyl of the ester product, RCH_2C(O)O (δ = 5.10 ppm) (see Supporting Information for typical spectra). When the initial concentration of aldehyde was held constant and the concentration of the catalytic precursor was varied over a ∼10-fold concentration range, a plot of reaction rate vs precatalyst concentration (Figure 2) indicates that the reaction is first-order dependent on precatalyst for both complexes. These results indicate that the best formulation of the active species in solution should be of monomeric nature. Keeping the catalyst concentration constant while varying the aldehyde over a ∼10-fold concentration range, a plot of reaction rates vs aldehyde concentration (Figure 3) indicates also a first-order kinetic dependence on aldehyde for both complexes.

Thus, the apparent rate law for the dimerization of aldehydes promoted by complexes **1** and **3** can be formulated as presented in eq 8.

$$v = k[\text{complex}]^1[\text{aldehyde}]^1 \qquad (8)$$

Since complex **3** is a highly coordinative unsaturated complex, it is expected that a limiting effective catalyst:substrate ratio will be operative. Hence, by measuring the reaction rate over a wide range of benzaldehyde concentrations while keeping the catalyst concentration constant, we have been able to determine that, as the ratio of benzaldehyde to catalyst **3** increases from 100 to ∼330, the rate of the reaction also increases; however, further increasing this ratio results in a decrease of the reaction rate (Figure 4). This suggests that, to obtain the fastest process, the preferential effective substrate:catalyst ratio lies around 300:1.

The influence of temperature on the reaction rate was investigated by repeating the same reaction at different temperatures while the concentrations of the catalyst and benzaldehyde

dx.doi.org/10.1021/ja105696p |*J. Am. Chem. Soc.* 2011, 133, 1341–1356

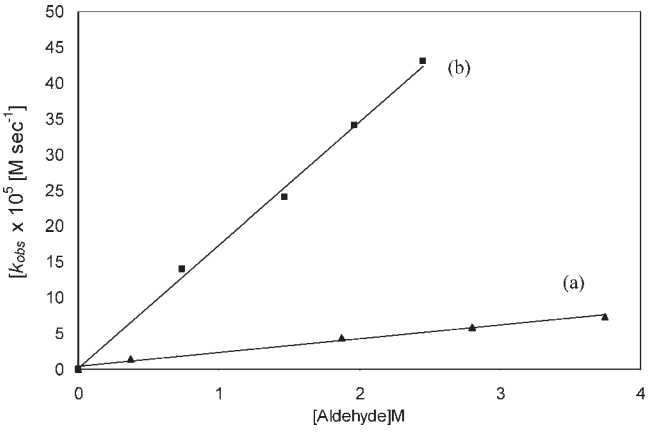

Figure 3. Observed aldehyde concentration-dependent reaction rate (k_{obs}) for the precatalysts (a) **1** and (b) **3**.

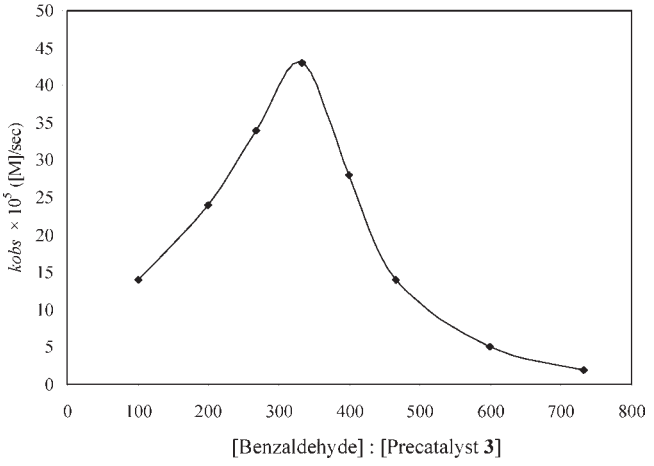

Figure 4. Variation of k_{obs} with the ratio between concentration of benzaldehyde and precatalyst **3** ([benzaldehyde] = 7.37 × 10^{-1}, 1.47, 1.97, 2.45, 2.94, 3.43, 4.41, and 5.39 M; [precatalyst **3**] = 7.37 × 10^{-3} M).

were kept constant. For both complexes **1** and **3**, similar kinetic dependences were observed on the aldehyde and the catalyst over the range of temperatures studied (35−95 °C). The derived activation parameters from Arrhenius and Eyring analysis are (error values are in parentheses) E_a = 7.16(4) kcal/mol, $\Delta H^{\ddagger}$= 6.58(4) kcal/mol, $\Delta S^{\ddagger}$ = −48.8(4) eu and E_a = 3.47(2) kcal/mol, $\Delta H^{\ddagger}$= 2.80(4) kcal/mol, $\Delta S^{\ddagger}$ = −65.2 (4)eu for complexes **1** and **3**, respectively. These results indicate that, as expected, the relatively more open coordinative complex **3** is more active than its congener complex **1**, and the significant negative $\Delta S^{\ddagger}$ value reveals a highly ordered metal-centered transition state for the hydride shift from the alkoxy ethereal ligands to the incoming benzaldehyde (*vide infra*, Figure 6 and Scheme 1). Moreover, the higher negative $\Delta S^{\ddagger}$ for complex **3** suggests a more organized transition state, which further supports a larger degree of coordinative unsaturation in complex **3** as compared to complex **1**.

Effect of the Substituent on the Thermodynamics Parameters. To evaluate the effect of substituents in the benzene ring on the dimerization reaction, the thermodynamic parameters (E_a, $\Delta H^{\ddagger}$, and $\Delta S^{\ddagger}$) of the rate-determining step (RDS) were also measured and calculated for the *meta*- and *para*-substituted benzaldehyde with the electron-withdrawing chlorine and the electron-donating methyl groups using complex **3** (Table 3 and Figure 5).

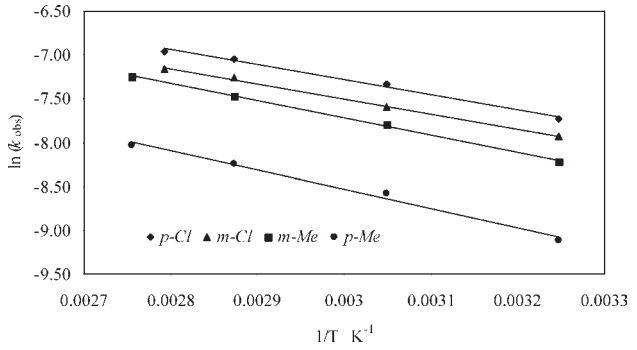

Figure 5. Arrhenius plot of the dimerization of (◆) *p*-chlorobenzaldehyde, (▲) *m*-chlorobenzaldehyde, (■) *m*-methylbenzaldehyde, and (●) *p*-methylbenzaldehyde by the complex **3**.

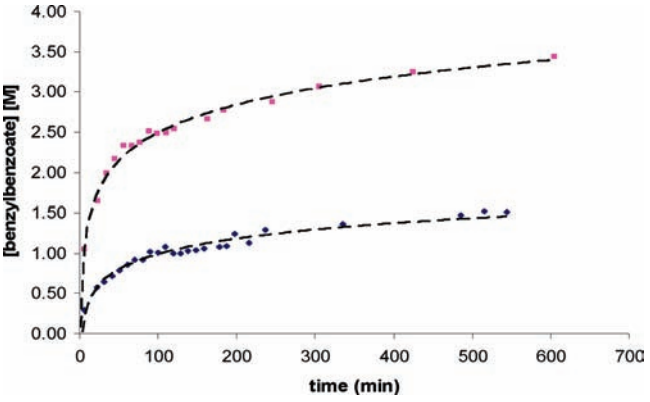

Figure 6. Kinetic isotopic effect on the Tishchenko reaction of benzaldehyde and α-d-benzaldehyde promoted by complex **1**.

Table 3 shows, in general, that the presence of an electron-withdrawing group at the aromatic ring induces a slight decrease in the E_a as compared to that for the substituted benzaldehyde with an electron-donating group. The difference in the enthalpy of activation for the different groups gives an important insight into the expected electron density in the metal at the RDS. The thermodynamic parameters for *ortho*-methyl- or -chloride-substituted benzaldehydes were not measured to avoid any steric factors that are probably equally or more predominate as compared to those observed in these cases (Table 1). For example, the extremely low reactivity of the *ortho*-tolualdehyde can be accounted for by the combined steric and electron effects hindering the approach of an aldehyde molecule to the metal−alkoxide bond. In the case of *ortho*-chlorobenzaldehyde, the steric effect does not appear to be a dominant effect; however, an additional electrostatic interaction between the metal and the chlorine atom may be operative.

In addition to the kinetic and thermodynamic studies, a primary isotopic effect was observed using α-deuterated benzaldehyde[30] with k_H/k_D = 2.7 for complex **1**, indicating that a hydride transfer is involved in the RDS (Figure 6). Stoichiometric reactions between the actinide complexes with benzaldehyde yield the expected stoichiometric amounts of $C_6H_5COOCH(CH_3)C_6H_5$, C_6H_5CO-$OCH(NEtMe)C_6H_5$, and $C_6H_5COOCH(C_4H_9)C_6H_5$, as measured by GC and GC/MS, when complexes **1**, **2**, and **3** were used, respectively. These results demonstrate that the aldehyde is able to insert into the initial actinide complexes, producing the active alkoxo species.

dx.doi.org/10.1021/ja105696p |*J. Am. Chem. Soc.* 2011, 133, 1341–1356

Scheme 1. Plausible Mechanism for the Catalytic Dimerization of Aldehyde by Organoactinide Complexes, Taking Complex 3 as a Representative Example

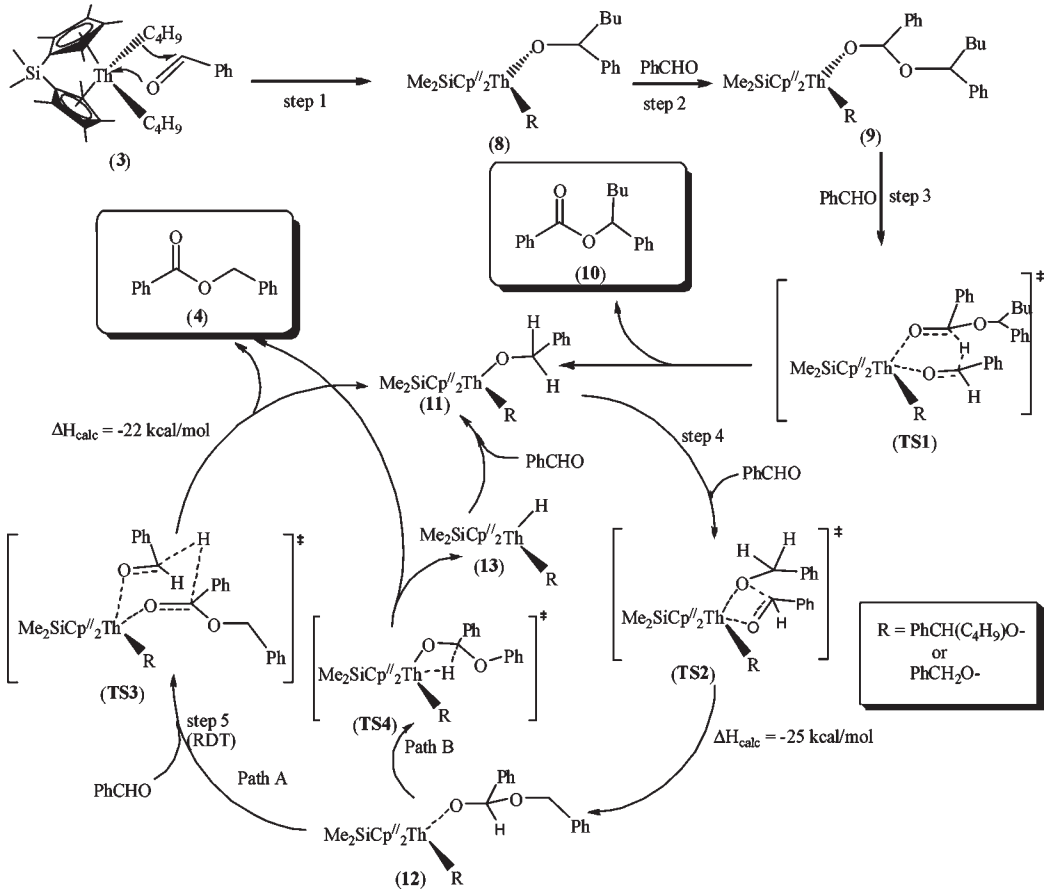

Stoichiometric Reactions. A few stoichiometric reactions were performed to gain some insight into the plausible mechanism of the reaction and to try to understand why only a dimer product is obtained. When complex **3** was reacted with 2 equiv of benzyl alcohol or n-butyl alcohol, the corresponding (bis)alkoxo complexes **3a** and **3b** were obtained (eq 9).

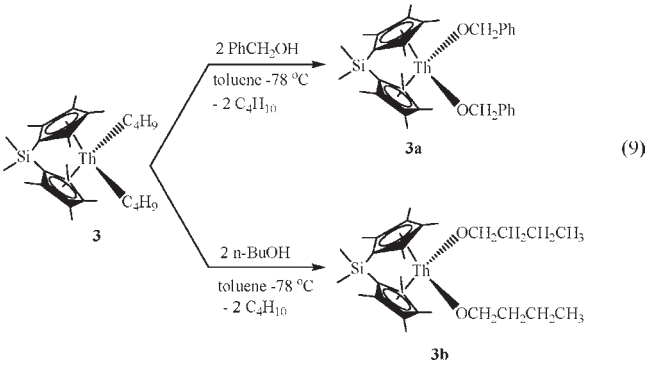

(9)

The reaction of complex **3a** with benzaldehyde produced the expected dimer product in a similar kinetic manner as with complex **3**. In addition, almost no reactivity was observed, at room temperature, for complex **3b** with butyraldehyde, as shown above for other aliphatic aldehydes. This result is indeed extremely informative since it indicates the stability of complex **3b** and the lack of a plausible β-H elimination pathway in the mechanism. Similar reactions with complex **1** produced the analogous complexes **1a** and **1b** with the same trends in reactivity as for complex **3**. In the stoichiometric reaction with complex **1a** or **1b**, the corresponding dimeric dihydride complex $((Cp^*_2ThH_2)_2)$ was not observed.[13d] Moreover, the reaction of complexes **1a** and **1b** with H_2 in pressure vessels did not produce the corresponding $(Cp^*_2ThH_2)_2$, again corroborating a pathway not involving the formation of a hydride intermediate.[13d,13f,23]

Table 3. Thermodynamic Data of Substituted and Unsubstituted Benzaldehyde during the Tishchenko Reaction with Precatalyst 3

substrate	E_a (kcal/mol)	$\Delta H^{\ddagger}$ (kcal/mol)	$\Delta S^{\ddagger}$ (eu)
benzaldehyde	3.47(4)	2.80(4)	−65.2(3)
m-chlorobenzaldehyde	3.45(4)	2.79(4)	−65.3(3)
p-chlorobenzaldehyde	3.41(4)	2.75(4)	−65.0(3)
m-methylbenzaldehyde	3.90(4)	3.24(4)	−64.4(3)
p-methylbenzaldehyde	4.36(4)	3.70(4)	−64.6(3)

DISCUSSION

Catalytic Dimerization of Aldehydes: Reaction Scope and Mechanism. The catalytic results for the selective dimerization of aldehydes promoted by complexes **1**, **2**, and **3** produced the

dx.doi.org/10.1021/ja105696p | J. Am. Chem. Soc. 2011, 133, 1341–1356

corresponding esters with high chemoselectivity without any other byproduct. It is worth mentioning here that, despite the fact that the actual catalytic species is not well defined, the observed trend of reactivity, **3** > **2** > **1**, might arise due to differences in coordinative unsaturation around the metal center. The presence of monodentate N-donor ligands with bulkier substituents in **2** sterically provides high shielding toward the metal center, while in **3** the *ansa*-type Cp″-bridged ligands open up the frontier orbitals, with the result that the Th center becomes more exposed to incoming substrates. This relation between the coordinative unsaturation and reactivity is consistent with previous observations for olefin insertion into M−R bonds[22] or the organoactinide catalytic hydroamination of alkynes.[33b] These results demonstrate the ability to scope the catalytic use of organoactinide complexes with oxygen-containing substrates and allow us to tailor the reactivity of these complexes in the Tishchenko reaction by modulating the spectator ancillary ligands. The lack of methane, EtMeNH, or butane using complexes **1**, **2**, or **3**, respectively, indicates that the aldehyde proton is not acting as a protonating agent, producing neither an acyl-type nor the dialkoxo metallacycle complex (eq 10).[31]

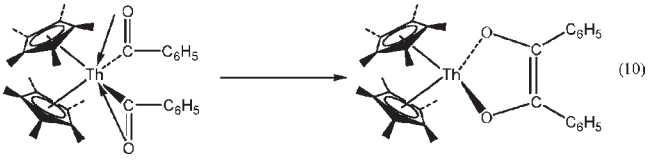

(10)

Moreover, in the reactions with benzaldehyde, the lack of stoichiometric amounts of methylbenzophenone, the amide $C_6H_5C(O)NEtMe$, or butylbenzophenone with complexes **1**, **2**, or **3**, respectively, indicates that, upon the insertion of the aldehyde into the Th−C or the Th−N bond, no concomitant β-H elimination is operative. Similar reactivity was also observed using the corresponding deuterium-benzaldehyde. Hence, it seems that a Th−H motif is not the main active moiety/intermediate in the reaction pathway with these organoactinides. When comparing the activities of these complexes as a function of a specific substrate, two major conclusions can be drawn: electron-withdrawing substituents at the aromatic ring induce better activities and the larger the coordinative unsaturation at the metal center, the higher the reactivity of the complex. Regarding the activity of the coordinatively unsaturated complex **3**, we were astonished to observe that it is able to support incipient reactivity moieties such as nitriles, methoxide, or even the nitro group.

It is important to point out that the lack of oligomeric compounds implies that, upon formation of the dimer, the termination (elimination of the ester) must be a thermodynamically driven process, avoiding any further additional insertions. Moreover, in the competition reaction, no statistical scrambling is observed, suggesting that the process is governed at the metal center and that no equilibrium or elimination of an already inserted aldehyde, if operative, is efficient. A plausible mechanism for the selective dimerization of aldehydes promoted by the organothorium complexes is presented in Scheme 1.

The mechanism consists of a sequence of well-known straightforward reactions such as an alkoxy formation via aldehyde insertion into a metal−carbon or metal−nitrogen σ-bond and σ-bond metathesis. The high oxophilicity of the thorium complexes initiates the catalytic process via the addition of two equivalents of aldehyde through a thermodynamically favored four-centered transition state (ΔH_{calc} = −68 kcal/mol), to give the corresponding bis(alkoxo) complex **8** (Scheme 1, step 1). The subsequent addition of aldehyde molecules into the thorium−alkoxide bond (Scheme 1, step 2) results in the formation of complex **9**. Complex **9** does not insert any additional aldehyde molecules but rather eliminates the first ester **10**, in stoichiometric amounts, presumably either via a hydride transfer to an incoming aldehyde through a six-centered transition state (Scheme 1, step 3, TS1), with the concomitant production of the active catalytic complex **11**, or via a β-H elimination and rapid insertion of an aldehyde to produce the active complex **11**. The catalytic cycle starts with the addition of an aldehyde molecule into the thorium−alkoxide bond of complex **11** (Scheme 1, step 4, TS2) in a similar manner to that in complex **3**, via a four-centered transition state, to produce complex **12**, which performs a hydride transfer to an additional aldehyde through a six-centered transition state as the RDS (Scheme 1, step 5, TS3), regenerating the active catalyst **11** and producing the final ester product **4**. Alternatively, a β-hydrogen elimination process from **12** may also generate the same ester products **4**, along with the formation of a Th−H complex **13** (Scheme 1, Path B, TS4), which potentially may react with an aldehyde to produce back the active catalytic species **11**. Interestingly, in step 2, β-hydrogen elimination is, in theory, also a plausible process to yield the corresponding Th−H moiety and the ketone, which indeed was not observed. Hence, it seems a rather difficult and extremely challenging process to convert a Th−O moiety into a Th−H motif. From a thermodynamic point of view, we have calculated the enthalpy of the reaction including a β-hydrogen elimination and found it to be energetically higher than the reaction via the six-centered transition state[32] (+56 and −47 kcal/mol, respectively, eqs 11−13).[32] Therefore, we suggest, on the basis of the thermodynamic calculations, the lack of stoichiometric methylbenzophenone, amide $C_6H_5C(O)NEtMe$, or butylbenzophenone for complexes **1**, **2**, or **3**, respectively, the observed deuterium isotope effect, and the stability of the bis(alkoxo) complexes, that if operative, β-hydrogen elimination should not be the main termination pathway.

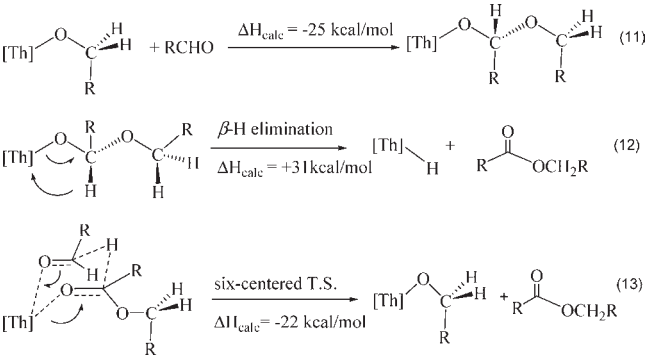

One important question that needs to be addressed regards the fact that no trimer or oligomers were obtained; however, the RDS is the elimination process via the six-centered transition state. When complex **11** reacts with an aldehyde, there is only one process that will yield complex **12**. Any hydride transfer from complex **11** to an incoming aldehyde, at this stage, will regenerate the same starting materials and hence will have no net effect on the reaction besides a kinetic delay. However, when an aldehyde approaches complex **12**, two possible pathways are feasible (Scheme 2). In the first pathway (a) an additional insertion may take place yielding complex **14**, whereas in the second (b) a hydride transfer will supply back the complex **11** and the ester product **4**. A substantiation indicating a greater preference for the hydride transfer as compared to an additional aldehyde insertion

dx.doi.org/10.1021/ja105696p | J. Am. Chem. Soc. 2011, 133, 1341–1356

Scheme 2. Two Possible Pathways for the Reaction of Benzaldehyde with Complex 12: (a) Addition to the Th−Alkoxo Bond via a Four-Centered Transition State and (b) Elimination of Ester Product via Hydride Transfer from the Alkoxo Ligand to the Incoming Benzaldehyde, Regenerating Catalytic Species 11

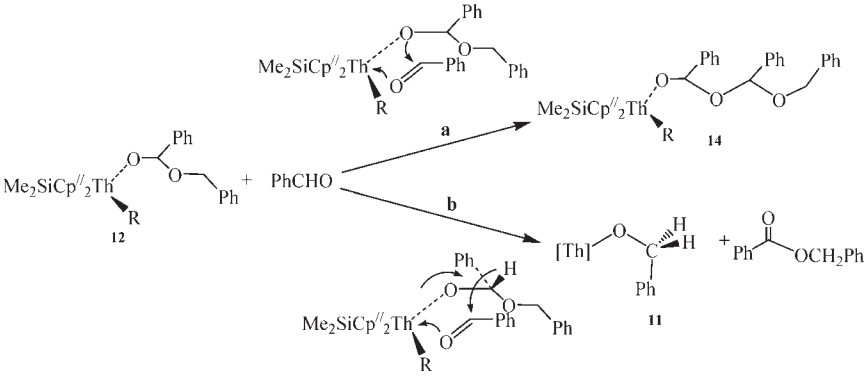

can be found in the entropy of activation. From the Eyring plots, the $\Delta S^{\ddagger}$ of activation for all studied aldehydes was calculated to be ~ -65 eu using complex **3** (Table 3). This result indicates a highly ordered transition state with considerable bond-making to compensate the bond-breaking. Thus, the process proceeds with a high degree of entropic reorganization on approaching the transition state. In contrast, for reactions in which a four-centered transition state is observed, a lower entropy of activation is acquired. For example, when complex **3** was utilized in the hydrosilylation of alkynes with $PhSiH_3$, the entropy of activation was found to be $-22.06(5)$ eu.[21e] Moreover, stoichiometric reactions were carried out to synthesize independently complex **14** from the reaction of the corresponding bisalkoxo complex and the aldehyde; however, complex **14** was never observed. Kinetically, the lack of formation of complex **14** is very peculiar. This result might indicate a plausible steric hindrance when an incoming aldehyde is approaching the metal center. For pathway a, when a four-centered transition state is forming, the benzylic carbon should reach a spatial position close to the oxygen atom bonded to the metal, inducing a tight transition state, whereas for pathway b, the benzylic carbon reaches a position close to the benzylic hydrogen, creating less hindrance between the incoming aldehyde and the alkoxo group. A comparison of the calculated E_a for pathway a (8.5 kcal/mol, see Figure 10) with the measured E_a (3.47 kcal/mol) for pathway b for benzaldehyde corroborates our findings that complex **11** and the corresponding dimer are the kinetic products when complex **12** reacts with an aldehyde and no oligomers are expected to be formed when $\Delta E_a > 5$ kcal/mol.

Since the reaction of the α-deuterated benzaldehyde did not yield another product besides the corresponding deuterated ester, since no deuterium was scrambled at the substrate or at the organometallic moiety, and since both reactions have the same reaction profile (Figure 6), we can calculate the energy of activation for the deuterated reaction using the probability kinetic equation (eq 14) in addition to the free energy $\Delta G^{\ddagger}$ for both processes.

$$\frac{k_H}{k_D} = e^{E_{aD} - E_{aH}/RT} \qquad (14)$$

where k_H and k_D are the first-order rate constants for the benzaldehyde and the α-deuterated benzaldehyde, respectively, and E_{aD} and E_{aH} are the energies of activation for the reaction of α-deuterated benzaldehyde and benzaldehyde, respectively.

For the reaction of α-deuterated benzaldehyde with complex **1**, the energy of activation was calculated as $E_{aD} = 7.74$ kcal/mol, with an enthalpy of activation of $\Delta H^{\ddagger}_D = 7.16$ kcal/mol, as well as the thermodynamic free energy of activations, $\Delta G^{\ddagger}_H = 21.12(4)$ kcal/mol and $\Delta G^{\ddagger}_D = 21.70(4)$ kcal/mol for benzaldehyde and deuterated benzaldehyde ($k_H/k_D \approx 2.7$), respectively. This kinetic difference between the deuterated and the nonlabeled benzaldehyde further supports that the RDS involves a hydride transfer to an incoming monomer.

As we have described in Scheme 1, the most probable RDS of the catalytic cycle is a hydride transfer from the organometallic moiety to an incoming aldehyde. Therefore, we expect that substituents with electron-withdrawing capabilities will enhance this process, and indeed this is observed (Table 1). Moreover, the E_a values for the different substituents exhibit the same trend, although there is not a very high difference between the *para* and *meta* substituents (Table 3). Hence, the reaction of two aldehydes competing for the active site is interesting. When two different aldehydes were reacted (benzaldehyde and *p*-Me-benzaldehyde) with different substrate feeds, the homodimer **4**, corresponding to benzaldehyde, was obtained always in larger yields. Benzaldehyde is expected to be more active than *p*-Me-benzaldehyde and hence will accept the hydride faster. When a larger amount of the *p*-Me-benzaldehyde was in the feed, the amounts of the esters were similar, indicating that, in principle, tailoring a product might be possible. In the case when benzaldehyde accepts the hydride transfer faster, the following insertion will indicate the preference for the addition between the two aldehydes (competing in a rapid step). Comparison of the amounts of products **4** and **7** in Table 2 reveals that the insertion of benzaldehyde is also partially preferred, since this competition occurs via a four-centered transition state.

When terephthalaldehyde was used, a polymer was obtained with DP = 25. Based on the mechanism proposed in Scheme 1, it is very plausible that the polymer is obtained by the consecutive insertions of esters having two aldehyde functional groups at the chain ends. Hence, the two chemoselective types of insertions are observed as depicted in eq 6.

At this point, DFT calculations were performed to find out the thermodynamically as well as kinetically most favored pathway of the reaction mechanism and to gain insight into the structure and bonding of various probable key intermediates/transition states that might be involved in the proposed catalytic cycle (Scheme 1). Calculations were performed with a model of the highly reactive

catalytic species **3**, but to minimize computational expense, the Cp″ moiety was replaced by Cp (C_5H_5), so the final calculated complex was $Me_2SiCp_2Th(C_4H_9)_2$ (**3′**), which should not have a major effect on the overall reaction course. Before doing any intense study, first we tried to validate the level of theory by comparing the geometry-optimized parameters of complex **3** with available crystal structure data for a closely related molecule, $Me_2SiCp''_2Th(CH_2SiMe_3)_2$,[13a] and we found an excellent match (1.5−2.5% deviation, see Supporting Information). For our calculations, the proposed catalytic cycle is divided into two parts: (a) activation of precatalyst **3** (Scheme 1, steps 1−3) and (b) the actual catalytic cycle (Scheme 1, steps 4 and 5 and Path B). During the course of the reaction, benzaldehyde molecules may approach the metal center in two different ways: (i) frontal approach between the two non-Cp ligands (Figure 7-i) or (ii) lateral approach between the Cp and non-Cp ligands (Figure 7-ii). We have found that the frontal approach (Figure 7-i) is the less energetic as well as the sterically more favored path.

The potential energy surface of the first part of the mechanism is shown in Figure 8. Insertion of two aldehyde molecules into the Th−C bond to form the Th−alkoxo complex **8′** was found to be very exothermic in nature, which is expected due to the high oxophilicity of the thorium atom. Subsequent addition of aldehydes to the Th−O bond is not highly exothermic but still is found to be an energetically favored process to form complex **9′**, which further reacts exothermically with another two moles of aldehyde to produce the catalytic species **11′** along with the elimination of the first ester product **10**. For this first part of the reaction mechanism, we were not concerned with the kinetic barriers for the various steps because our prime interest lies in the actual catalytic cycle, and indeed the formation of the actual catalytic species was found to be a highly thermodynamically driven process (Figure 8).

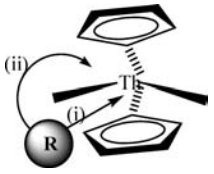

Figure 7. Possible paths for benzaldehydes to approach the metal center during the course of the reaction: (i) frontal approach and (ii) lateral approach.

The actual catalytic cycle (Scheme 1, steps 4 and 5) has been studied explicitly considering the two possible termination pathways: (a) via a six-centered hydride-transfer transition state (Scheme 1, TS3) or (b) through a β-hydride elimination process (Scheme 1, TS4). For calculation efficiency, we have investigated at any time only one aldehyde insertion into the Th−O bonds of the various catalytic species, and the energy profile diagram is shown in Figure 9. In the first step, insertion of an aldehyde molecule into the Th−alkoxo bond of the catalytic species **11′** takes place via a highly ordered four-centered transition state (Figure 9, TS2), with a kinetic barrier of +6.0 kcal/mol, to form the unsymmetrical alkoxo-ether intermediate **11′a**, which may undergo an addition of another aldehyde via a similar four-centered transition state (Figure 9, TS2a), to produce the symmetrical Th−bis(alkoxo) intermediate **12′**, or hydride transfer may take place from the alkoxo ligand to the incoming benzaldehyde via a six-centered transition state (Figure 9, TS3), to regenerate the catalytic species **11′** along with the elimination of the dimeric ester product **4**. At this stage, the kinetic barriers of 6.3 and 13.5 kcal/mol for TS2a and TS3, respectively, favor the formation of **12′** over regeneration of **11′**. However, the addition of another aldehyde to **12′** may again lead to the regeneration of complex **11′** via the six-centered transition state (Figure 9, TS3a, +13.7 kcal/mol). Therefore, the calculated activation barriers for the transition-state structures TS2a, TS3, and TS3a (Figure 9) suggest that, during the course of the reaction, there may be an equilibrium between species **11′a** and **12′**, and considering the steric hindrance, regeneration of the active catalytic species **11′a** along with elimination of ester product **4** might preferably take place from **11′a**. Alternatively, β-hydrogen elimination from the alkoxo-ether ligand on **11′a** or **12′** may also produce the dimeric ester product **4**, along with the formation of the Th−hydride intermediates **13′a** and **13′** (Figure 9, Path B), which with additional aldehyde insertions will regenerate the catalytic species **11′**. These pathways, as seen in Figure 9, are energetically unfavorable, leading to the formation of thermodynamically highly

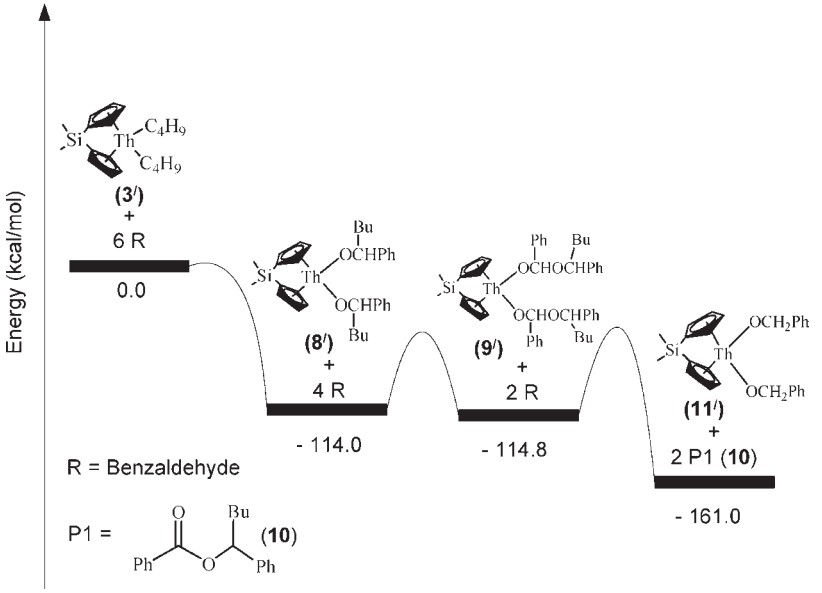

Figure 8. Potential energy surface for the formation of active catalytic species **11′** (model of **11**) from precatalyst **3′** (model of **3**).

dx.doi.org/10.1021/ja105696p | *J. Am. Chem. Soc.* 2011, 133, 1341–1356

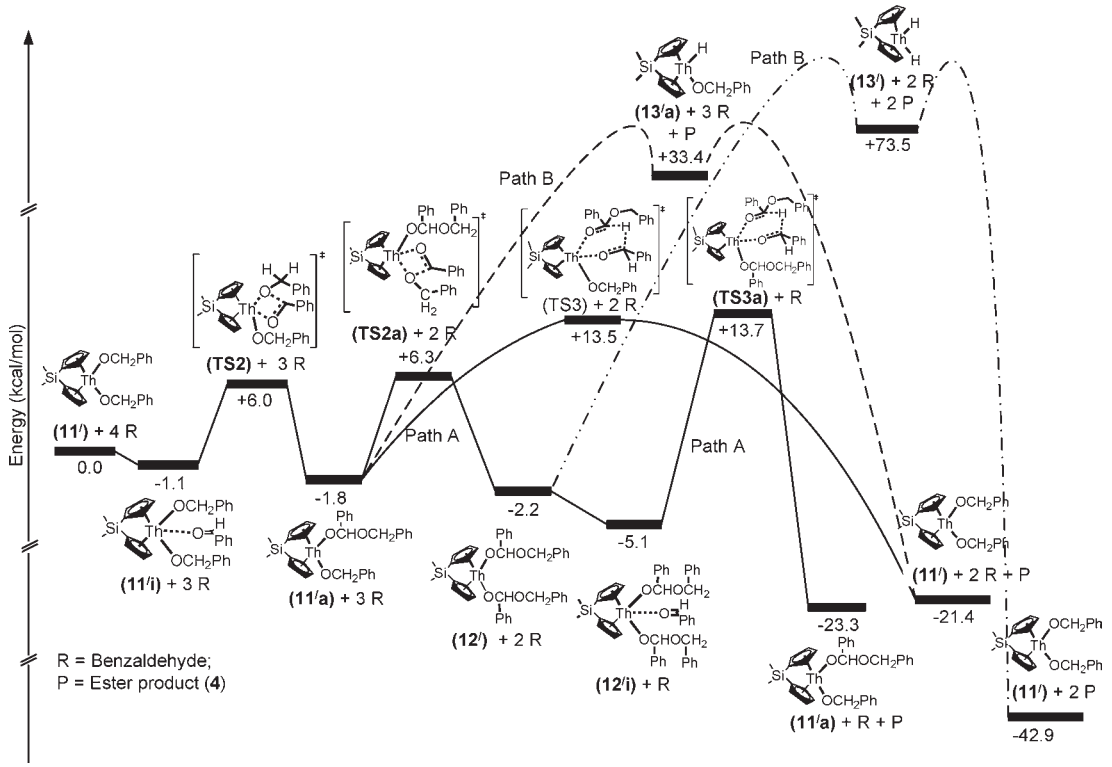

Figure 9. Potential energy surface for the possible pathways in the catalytic cycle.

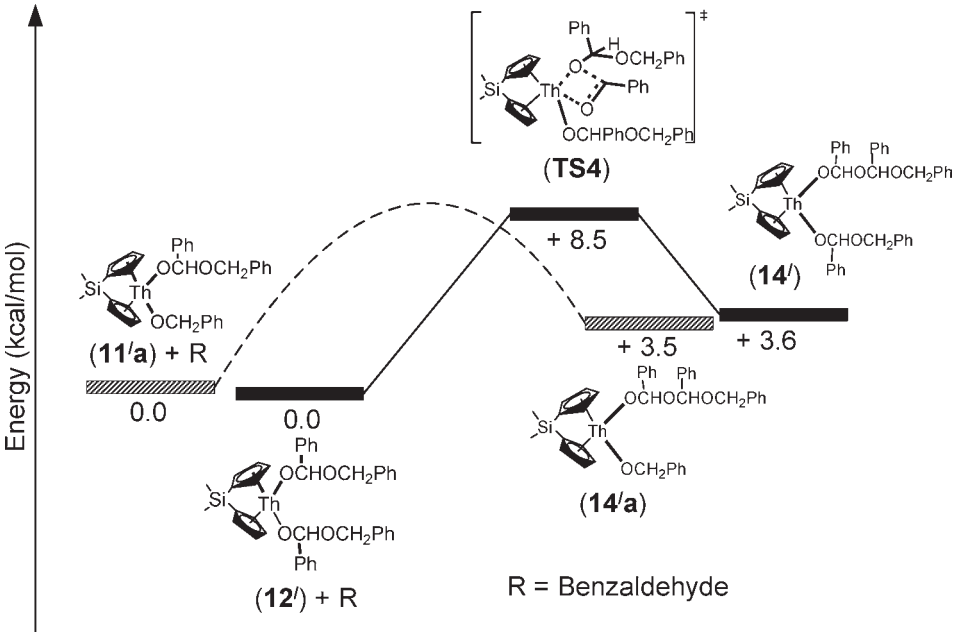

Figure 10. Potential energy surface for the third addition of benzaldehyde across the Th−O bond of catalytic intermediates **11′a** and **12′**.

unstable Th−hydride intermediates, **13′a** and **13′**, and may have even higher kinetic barriers. Therefore, in the catalytic cycle, the β-hydrogen elimination step is quite unlikely. It is worth mentioning here that, in each step of the reaction mechanism, prior to the addition of aldehydes to the Th−O bonds in **11′** and **12′** a slightly stable aldehyde adduct (Figure 9, **11′i** and **12′i**) has been observed, evident of the high oxophilicity of the Th motif, which is probably the main driving force of the reaction.

Interestingly, the calculated energy profile diagram (Figure 10) for the third addition of benzaldehyde to the intermediate species **12′** or to **11′a** reveals that the kinetic barrier for the process is not much higher (+3.5 kcal/mol); however, the intermediates formed, **14′** or **14′a** (Figure 10), are thermodynamically unstable. Therefore, this is more likely to be a thermodynamically controlled process rather than kinetically controlled, and hence addition of a third mole of benzaldehyde across the

dx.doi.org/10.1021/ja105696p |*J. Am. Chem. Soc.* 2011, 133, 1341–1356

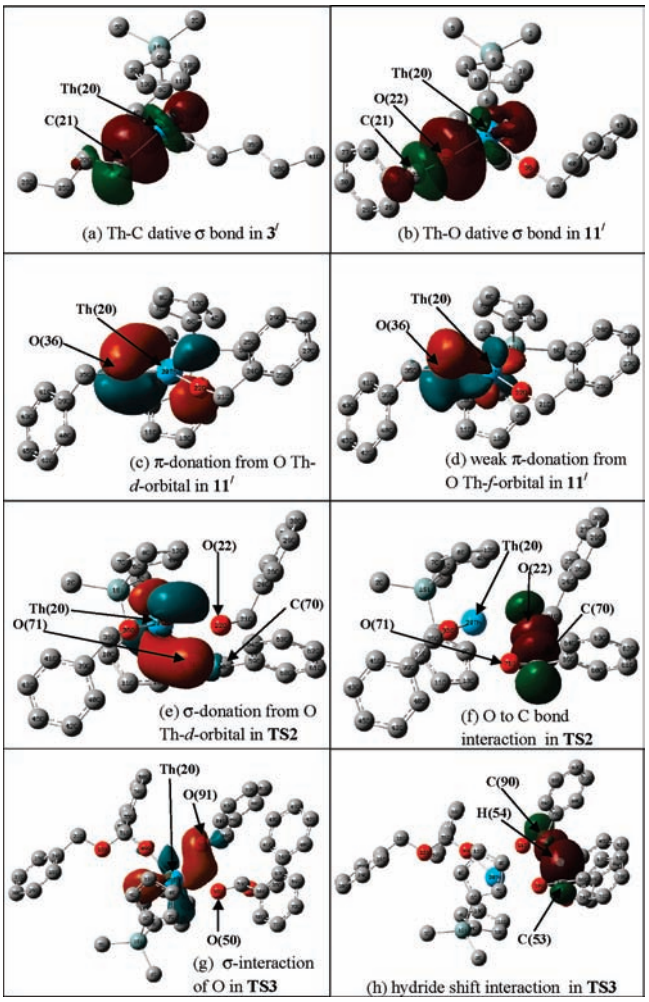

Figure 11. Various molecular orbitals obtained during bond formation in different spcies in the catalytic cycle: (a) dative σ-bond formation between C of the butyl ligand and Th in the precatalyst **3′**; (b) dative σ-bond formation between O of the alkoxo ligand and Th in the precatalyst **11′**; (c) π-donation from O of the alkoxo ligand p-orbital to the Th d-orbital in **12′** (similar donation also observed for **12′**); (d) weak π-donation from O of the alkoxo ligand p-orbital to the Th f-orbital in **11′** (similar donation also observed for **12′**); (e) σ-donation from the sp hybrid orbital of O of incoming benzaldehyde to the Th d-orbital in **TS2**; (f) lone-pair donation from O of the alkoxo ligand to the LUMO of the carbonyl carbon atom of incoming benzaldehyde in **TS2**; (g) σ-donation from the sp hybrid orbital of O of incoming benzaldehyde to the Th d-orbital in **TS3**; (h) donation of a C−H bond pair to the LUMO of the carbonyl carbon atom of incoming benzaldehyde in **TS3**.

Th−O bond is unlikely, which is in agreement with the experimental results.

To gain insight into the electronic behavior of various intermediate complexes as well as formation of transition states (Scheme 1), Natural Bond Orbital (NBO) analyses were carried out, and in the following section we mainly discuss the bonding interaction between non-Cp ligands and the Th center in various catalytic species, skipping the well-established bonding of the $[(C_5H_5)_2An]^+$ fragment. In complex **3′**, the $\sigma_{Th-C(butyl)}$ bond is formed by 85% contribution from the ligand C-hybrid orbital (72% p-character) and 15% contribution of the metal hybrid orbital, which consists of 69% d-character along with a significant contribution of 12% f-character (Figure 11a). In complex **11′**, a metal−ligand bond is found to form by the dative σ_{Th-O} interaction, which has about 94% ligand orbital contribution due to the σ donation from the O hybrid orbital of 64% s- and 36% p-character toward the metal hybrid orbital having 91% d- and 7% f-character (Figure 11b).

Similarly, in the complex **12′**, the σ-donation from the O hybrid orbitals (61% s- and 39% p-character) to Th hybrid orbitals (90% d- and 8% f-character) leads to the formation of the dative σ_{Th-O} bond. In complexes **11′** and **12′**, apart from the dative σ-donation, a significant π-donation is also observed from the O lone pair (pure p-character) to the symmetry-adapted vacant d-orbital of the metal center (Figure 11c) and a weaker donation from the p-orbital of the O atom to the vacant symmetry-adapted f-orbital of the metal (Figure 11d). It is worth mentioning here that, in comparison to complexes **11′** and **12′**, precatalyst **3′** shows a higher degree of metal orbital participation (15%), with around 12% f-orbital contribution in the Th−ligand (non-Cp) interaction, indicating greater covalency.

Some very interesting subtleties can be found in support of the formation of four- and six-centered transition states (Scheme 1, TS2 and TS3). During the formation of the four-centered transition states, as the aldehyde molecule approaches the metal center (2.47 Å), a bond-forming interaction has been observed, resulting from significant donation of electron density from the O lone pair (O(71), Figure 11e) of the sp-hybrdized orbital (54% s- and 46% p-character) to the antibonding metal hybrid orbital (89% d- and 10% f-character) (Figure 11e). At the same time, weakening of the dative σ-donation of the Th−alkoxo bond is observed; consequently, the Th−O bond length (Th(20)−O(22), Figure 11e) increases to 2.41 Å from 2.15 Å in **11′**. Another strong donation is observed from the lone pair of the alkoxo oxygen (O(22), Figure 11f) (84% p-character) to the lowest unoccupied molecular orbital (LUMO) of the carbonyl carbon (p-orbital) (C(70), Figure 11f) of the incoming benzaldehyde. It was interesting to observe a significant drift of electron density from the C(70)−O(71) bond pair of the incoming benzaldehyde to the metal vacant d-orbital, which further supports weakening of the C−O double bond character with simultaneous bond-forming interaction between the O atom (O(71)) and the Th metal center. The NBO population analysis of the transition state (TS2) indicates an increase in electron density (natural) on the Th atom from +2.05 for **11′** to +1.88 in TS2 due to donation of more electron density from the incoming benzaldehyde, while drift of electron density from the alkoxo O atom (O22, Figure 11e,f) to the aldehydic carbon (C(70)) results in the decreases of electron density in O(22) from −0.874 for **11′** to −0.772 in TS2. In TS2, an increase in electron density on the aldehydic C atom (C(70)) was expected, as it received electron density from the alkoxo O atom (O(22)), but in contrast, it decreases from +0.394 for pure benzaldehyde to +0.452, while on the O atom of the interacting benzaldehyde it increases from −0.529 for pure benzaldehyde to −0.677. This discrepancy may not be unusual, as there is a strong net drift of electron density from the aldehydic unit (O lone pair as well as C−O bond pair) to the Th metal center. These observations clearly indicate new bond-forming interactions between Th and O of the incoming benzaldehyde and between the alkoxo oxygen of the ligand and the benzaldehyde C atom, as well as simultaneous bond-breaking/weakening interaction of the Th−alkoxo bond in this four-centered transition state (Figure 11e,f).

During the formation of the six-centered transition states (TS3 and TS3a), the incoming benzaldehyde shows a similar type of interaction toward the metal center as in the four-centered

dx.doi.org/10.1021/ja105696p | J. Am. Chem. Soc. 2011, 133, 1341–1356

transition states. A strong donation for a bond-forming interaction is observed from the O lone pair of the incoming benzaldehyde to the antibonding metal hybrid orbital (84% d- and 12% f-character) (O(91)−Th(20), Figure 11g). It is interesting to note that the O lone pair is in an sp-hybrdized orbital rather than in a pure p-orbital, which further indicates weakening of the C−O double-bond character in the incoming benzaldehye unit. A significant decrease in the dative σ-donation and almost absence of π-donation from the alkoxo O atom of the ligand (involved in TS3 and TS3a formation) to the metal center is observed, and consequently the Th−alkoxide bond length increases to 2.42 Å in TS3 (2.41 Å in TS3a) from 2.17 Å in complex **12′**. Apart from these, the expected hydride shift is well evident from a strong donation of the C(53)−H(54) bond pair toward the LUMO of the carbonyl carbon (C(90), Figure 11h) of the incoming benzaldehyde.

CONCLUSIONS

The results presented in this study have opened a new window in the field of catalytic activities of organoactinide complexes containing oxygenated substrates. The main feature is the unexpected activation of thorium−alkoxide bonds, which was believed to be a dead-end in organoactinide chemistry. We have found that the complexes **1**−**3** are active for the dimerization of aldehydes with the organoactinide complex $Me_2SiCp''_2ThBu_2$ (**3**), having high activity and, more surprisingly, allowing the dimerization of substrates like furanaldehyde, cyanobenzaldehyde, and nitrobenzaldehyde. To our knowledge, this is the first example of a catalytic process for actinide complexes in which such types of functional groups have been part of a substrate.

The lower values of E_a and $\Delta H^{\ddagger}$, and the much lower negative value of $\Delta S^{\ddagger}$, obtained for complex **3** as compared to those obtained for complex **1** clearly indicate the positive impact of obtaining a more coordinatively unsaturated complex by introducing the bridging ligand. However, at the same time, we were surprised that the more active complex also allowed the more reactive substrates to undergo chemoselective processes without any decomposition or formation of different catalytic products.

Our vision to induce organoactinide complexes to be active toward substrates containing a nucleophilic motif was based on developing a thermoneutral reaction. Since actinides are expected to undergo metathesis-type reactions, following a four-centered transition state, a reaction in which the same type of metal−moiety bonds are made and broken is expected to exhibit this requirement to a good extent. Hence, if this is achieved, the reaction will be directed by entropy parameters, and taking into account the enthalpy of the reaction, we can anticipate that a new catalytic process will be afforded.

MATERIALS AND METHODS

All manipulations of air-sensitive materials were performed with the rigorous exclusion of oxygen and moisture in flamed Schlenk-type glassware on a dual-manifold Schlenk line, or interfaced to a high vacuum (10^{-5} Torr) line, or in a nitrogen-filled Vacuum Atmospheres glovebox with a medium-capacity recirculator (1−2 ppm O_2). Argon and nitrogen were purified by passage through a MnO oxygen-removal column followed by a 4 Å molecular sieve column. All the solvents, benzene-d_6, THF-d_8, and toluene-d_8, were distilled under nitrogen from Na/K alloy. Hydrocarbon solvents for vacuum line manipulations were stored in vacuo over Na/K alloy in resealable bulbs. The syntheses of $(Cp^*)_2ThMe_2$ (**1**), $Th\{N(CH_3)CH_2CH_3\}_4$ (**2**), and $Me_2SiCp''_2ThBu_2$ (**3**) were done according to published methods.[13a,33] Benzaldehyde, *o*-tolualdehyde, *m*-tolualdehyde, *p*-tolualdehyde, *o*-furaldehyde, acetaldehyde, phenylacetaldehyde, valeraldehyde, and cyclohexanaldehyde (Aldrich) were distilled over sodium bicarbonate and stored inside a glovebox. *p*-Chlorobenzaldehyde, *o*-nitrobenzaldehyde, *m*-nitrobenzaldehyde, and *p*-nitrobenzaldehyde (Aldrich) were crystallized from a 1:3 mixture of $EtOH/H_2O$, sublimed, and stored in glovebox.

NMR spectra were recorded on Avance 500 and Avance 300 Bruker spectrometers. Chemical shifts for ^1H and ^{13}C are referenced to internal solvent resonances and are reported relative to tetramethylsilane. All reactions monitored by NMR were performed in J. Young Teflon valve-sealed NMR tubes. GC/MS experiments were conducted in a GC/MS (Finnigan Magnum) spectrometer with a J&W DB5 column (30 m × 250 μm).

Synthesis of $Me_2SiCp''_2Th(OCH_2C_6H_5)_2$ (3a). Under an argon flush, 0.65 mL (6.2 mmol) of $C_6H_5CH_2OH$ was syringed into a 50-mL Schlenck flask containing a magnetic stir bar and a solution of 2 g (3.10 mmol) of $Me_2SiCp''_2ThBu_2$ cooled at −78 °C. The mixture was stirred for 1 h, and the solvent was replaced by 15 mL of hexane, keeping the solution cold at all times. Cold filtration (−78 °C) afforded a white precipitate. Yield: 1.82 g (0.82%). ^1H NMR (300 MHz, C_6D_6): δ 0.67 (s, 6H), 1.78 (s, 12H, Cp″), 2.10 (s, 12H, Cp″), 3.64 (s, 4H), 6.45−722 (m, 10H) Anal. Calcd for $C_{34}H_{44}O_2SiTh$: C, 54.83; H, 5.95. Found: C, 54.90;H, 5.91.

Synthesis of $Me_2SiCp''_2Th(O^nBu)_2$ (3b). Under an argon flush, 0.68 mL (6.2 mmol) of ^{n}BuOH was syringed into a 50-mL Schlenck flask containing a magnetic stir bar and a solution of 2 g (3.10 mmol) of $Me_2SiCp''_2ThBu_2$ cooled at −78 °C. The mixture was stirred for an additional hour, and the solvent was replaced by 15 mL of hexane, keeping the solution cold at all times. Cold filtration (−78 °C) afforded a white precipitate. Yield: 1.57 g (0.75%). ^1H NMR (300 MHz, C_6D_6): δ 0.72 (s, 6H), 1.01 (t, J = 12 Hz, 6H, CH_2CH_3), 1.33 (m, 4H), 1.48 (m, 4H), 1.97 (s, 12H, Cp″), 2.17 (s, 12H, Cp″), 3.53 (t, J = 12 Hz, 4H) Anal. Calcd for $C_{28}H_{48}O_2SiTh$: C, 49.69; H, 7.15. Found: C, 49.20; H, 7.39.

Tishchenko Reaction: General Procedure. In a glovebox, a J. Young NMR tube was charged with one of the complexes **1**−**3** (0.01 mmol), dissolved in 50−100 μL of NMR solvent (toluene-d_8/benzene-d_6). To the solution was added 0.98 mmol of the corresponding aldehyde, and the mixture was then immediately diluted to 500 μL with toluene-d_8/benzene-d_6. The progress of the reaction was monitored continuously with the help of ^1H NMR. After 24−48 h, the tube was opened to air and the reaction quenched with methanol. The products were identified by NMR and GC/MS analysis of the crude reaction mixture.

Esterification of Benzaldehyde. Dimerization of benzaldehyde to produce benzyl benzoate was carried out with 100 μL of benzaldehyde (0.98 mmol) and 0.01 mmol of complex **1**, **2**, or **3** following the general procedure described above. The benzyl benzoate was obtained exclusively in 65 and 85% yield for complexes **1** and **2**, respectively, after 48 h, while for complex **3**, a 96% yield was observed after 24 h of reaction.

Characterization Data for Benzyl Benzoate. ^1H NMR (500 MHz, C_6D_6): δ 5.14 (s, 2H, -CH_2), 7.21−7.01 (m, 8H, Ph), 8.04 (d, J = 7.7 Hz, 2H, Ph). ^{13}C NMR (125 MHz, C_6D_6): δ 68.4, 129.9, 130.1, 130.3, 130.5, 131.9, 132.6, 134.8, 138.5, 167.6. MS: m/z 212 (M^+), 105 ($PhCO^+$), 91 ($PhCH_2^+$).

Esterification of *p*-Tolualdehyde. The esterification product (4′-methylbenzyl)-4-methylbenzoate was obtained by the dimerization of 4-methylbenzaldehyde (0.98 mmol) in the presence of 0.01 mmol of complex **1**, **2** or **3** following the general procedure described above. The product was obtained exclusively in 65 and 82% yield for complexes **1** and **2**, respectively, after 48 h, while for complex **3**, a 74% yield was observed after 24 h of reaction.

Characterization Data for (4′-Methylbenzyl)-4-methylbenzoate. ^1H NMR (500 MHz, C_6D_6): δ 1.84 (s, 3H, -CH_3), 1.93 (s, 3H, -CH_3),

5.08 (s, 2H, -CH_2), 6.74 (d, J = 7.7 Hz, 2H, Ph), 6.83 (d, J = 7.7 Hz, 2H, Ph), 7.08 (d, J = 7.7 Hz, 2H, Ph), 7.98 (d, J = 7.7 Hz, 2H, Ph). ^{13}C NMR (125 MHz, C_6D_6): δ 22.5, 22.8, 68.0, 130.2, 130.4, 130.8, 130.9, 131.5, 135.3, 139.3, 144.9, 167.7. MS: m/z 240 (M^+), 119 ($ArCO^+$), 105 ($ArCH_2^+$), 91 ($MePh^+$).

Esterification of *m*-Tolualdehyde. The esterification product (3′-methylbenzyl)-3-methylbenzoate was obtained by the dimerization of 3-methylbenzaldehyde (0.98 mmol) in the presence of 0.01 mmol of complex **1**, **2**, or **3** following the general procedure described above. The product was obtained exclusively in 20 and 75% yield for complexes **1** and **2**, respectively, after 48 h, while for complex **3**, 94% yield was observed after 24 h of reaction.

Characterization Data for (3′-Methylbenzyl)-3-methylbenzoate. ^{1}H NMR (500 MHz, C_6D_6): δ 1.96 (s, 3H, -CH_3), 2.04 (s, 3H, -CH_3), 5.21 (s, 2H, -CH_2), 6.90−7.05 (m, 6H, Ph), 8.00−8.01 (m, 2H, Ph). ^{13}C NMR (125 MHz, C_6D_6): δ 20.9, 21.2, 66.9, 125.9, 127.4, 128.6, 128.8, 129.1, 129.5, 130.6, 130.8, 133.9, 136.7, 138.3, 138.4, 166.3. MS: m/z 240 (M^+), 119 ($ArCO^+$), 105 ($ArCH_2^+$), 91 ($MePh^+$).

Esterification of *o*-Tolualdehyde. The esterification product (2′-methylbenzyl)-2-methylbenzoate was obtained by the catalytic dimerization of 0.98 mmol of 2-methylbenzaldehyde and 0.01 mmol of complex **1**, **2**, or **3** following the general procedure described above. The product was obtained exclusively in 10 and 50% yield for complexes **1** and **2**, respectively, after 48 h, while for complex **3**, 70% yield was observed after 24 h of reaction.

Characterization Data for (2′-Methylbenzyl)-2-methylbenzoate. ^{1}H NMR (500 MHz, C_6D_6): δ 2.07 (s, 3H, -CH_3), 2.58 (s, 3H, -CH_3), 5.17 (s, 2H, -CH_2), 6.88−7.02 (m, 6H, Ph), 7.24 (d, J = 7.5 Hz, 1H, Ph), 7.98 (d, J = 7.5 Hz, 1H, Ph). ^{13}C NMR (125 MHz, C_6D_6): δ 18.9, 22.0, 65.0, 126.0, 126.4, 126.5, 128.8, 129.9, 130.8, 131.6, 132.2, 132.7, 134.9, 137.5, 141.0, 167.1. MS: m/z 240 (M^+), 119 ($ArCO^+$), 105 ($ArCH_2^+$), 91 ($MePh^+$).

Esterification of *p*-Chlorobenzaldehyde. The esterification product (4′-chlorobenzyl)-4-chlorobenzoate was obtained by the reaction of 0.98 mmol of 4-chlorobenzaldehyde and 0.01 mmol of complex **1**, **2**, or **3** following the general procedure described above. The product was obtained exclusively in 60, 85, and 98% yield for complexes **1**, **2**, and **3**, respectively, after 24 h of reaction.

Characterization Data for (4′-Chlorobenzyl)-4-chlorobenzoate. ^{1}H NMR (500 MHz, C_6D_6): δ 4.79 (s, 2H, -CH_2), 7.65 (d, J = 9.2 Hz, 2H, Ph), 6.91 (d, J = 9.2 Hz, 2H, Ph), 6.85 (d, J = 9.0 Hz, 2H, Ph), 6.73 (d, J = 9.0 Hz, 2H, Ph). ^{13}C NMR (125 MHz, C_6D_6): δ 65.1, 129.3, 128.6, 130.0, 130.2, 131.5, 136.1, 134.9, 139.5, 165.0. MS: m/z 280 (M^+), 139 ($ArCO^+$), 125 ($ArCH_2^+$).

Esterification of *m*-Chlorobenzaldehyde. Dimerization of 3-chlorobenzaldehyde to produce (3′-chlorobenzyl)-3-chlorobenzoate was carried out by mixing 0.98 mmol of the aldehyde with 0.01 mmol of complex **1**, **2**, or **3** following the general procedure described above. The product was obtained exclusively in 50, 80, and 95% yield for complexes **1**, **2**, and **3**, respectively, after 24 h of reaction.

Characterization Data for (3′-Chlorobenzyl)-3-chlorobenzoate. ^{1}H NMR (500 MHz, C_6D_6): δ 4.85 (s, 2H, -CH_2), 8.06 (s, 1H, Ph), 7.73 (d, J = 9.0 Hz, 1H, Ph), 7.14 (s, 1H, Ph), 7.01 (t, J = 7.8 Hz, 1H, Ph), 6.75 (d, J = 9.0 Hz, 1H, Ph), 6.61−6.77 (m, 3H, Ph). ^{13}C NMR (125 MHz, C_6D_6): δ 66.5, 128.3, 129.1, 131.0, 131.5, 130.6, 135.4, 136.7, 140.5, 166.0. MS: m/z 280 (M^+), 139 ($ArCO^+$).

Esterification of *o*-Chlorobenzaldehyde. The esterification product (2′-chlorobenzyl)-2-chlorobenzoate was obtained by the reaction of 0.98 mmol of 2-chlorobenzaldehyde and 0.01 mmol of complex **1**, **2**, or **3** following the general procedure described above. The product was obtained exclusively in 57, 78, and 89% yield for complexes **1**, **2**, and **3**, respectively, after 24 h of reaction.

Characterization Data for (2′-Chlorobenzyl)-2-chlorobenzoate. ^{1}H NMR (500 MHz, C_6D_6): δ 5.30 (s, 2H, -CH_2), 7.64 (d, J = 8.4 Hz, 1H, Ph), 7.07 (t, J = 8.4 Hz, 2H Ph), 6.86 (dd, 2H, Ph), 6.61−6.74 (m, 3H, Ph). MS: m/z 280 (M^+).

Esterification of *p*-Methoxybenzaldehyde. The esterification product (4′-methoxybenzyl)-4-methoxybenzoate was obtained by the dimerization of 0.98 mmol of 4-methoxybenzaldehyde in the presence of 6.5 mg (0.01 mmol) of complex **3** as catalyst following the general procedure described above. The product was obtained exclusively in 22% yield (NMR) after 12 h of reaction.

Characterization Data for (4′-Methoxybenzyl)-4-methoxybenzoate. ^{1}H NMR (500 MHz, C_6D_6): δ 5.20 (s, 2H, -CH_2), 3.15 (s, 3H, -CH_3), 3.03 (s, 3H, -CH_3) 6.51 (d, J = 8.7 Hz, 2H, Ph), 6.61 (d, J = 8.7 Hz, 2H, Ph), 7.08 (d, J = 7.8 Hz, 2H, Ph), 8.03 (d, J = 7.8 Hz, 2H, Ph). ^{13}C NMR (125 MHz, C_6D_6): 57.2, 66.3, 115.2, 125.3, 129.7, 132.6, 136.1, 160.9, 168.0. MS: m/z 272 (M^+).

Esterification of *p*-Cyanobenzaldehyde. The esterification product (4′-cyanobenzyl)-4-cyanobenzoate was obtained by the reaction of 0.98 mmol of 4-cyanobenzaldehyde and 6.5 mg (0.01 mmol) of the catalyst **3** following the general procedure described above. The product was obtained exclusively in 86% yield (NMR) after 12 h of reaction.

Characterization Data for (4′-Cyanobenzyl)-4-cyanobenzoate. ^{1}H NMR (500 MHz, $CDCl_3$): δ 5.47 (s, 2H, -CH_2), 8.22 (d, J = 6.0 Hz, 2H, Ph), 7.80 (d, J = 9.0 Hz, 2H, Ph), 7.74 (d, J = 9.0 Hz, 2H, Ph), 7.58 (d, J = 6.0 Hz, 2H, Ph). ^{13}C NMR (125 MHz, $CDCl_3$): δ 66.2, 116.8, 117.8, 118.3, 128.4, 130.2, 132.3, 132.5, 134.3, 140.5, 165.2. MS: m/z 262 (M^+), 131 ($ArCO^+$), 90 ($ArCH_2^+$).

Esterification of *p*-Nitrobenzaldehyde. The esterification product (4′-nitrobenzyl)-4-nitrobenzoate was obtained by the reaction of 0.98 mmol of 4-nitrobenzaldehyde and 6.5 mg (0.01 mmol) of the catalyst **3** following the general procedure described above. The product was obtained exclusively in 51% yield (NMR) after 6 h of reaction.

Characterization Data for (4′-Nitrobenzyl)-4-nitrobenzoate. ^{1}H NMR (500 MHz, $C_6D_5CD_3$): δ 4.70 (s, 2H, -CH_2), 7.70 (d, J = 9.0 Hz, 2H, Ph), 7.52 (d, J = 9.0 Hz, 2H, Ph), 7.28 (d, J = 9.0 Hz, 2H, Ph), 6.72 (d, J = 9.0 Hz, 2H, Ph). ^{13}C NMR (125 MHz, $C_6D_5CD_3$): δ 67.1, 117.7, 118.6, 130.6, 131.4, 166.2. MS: m/z 302 (M^+), 151 ($ArCO^+$), 137 ($ArCH_2^+$).

Esterification of *m*-Nitrobenzaldehyde. The esterification product (3′-nitrobenzyl)-3-nitrobenzoate was obtained by the reaction of 0.98 mmol of 3-nitrobenzaldehyde and 6.5 mg (0.01 mmol) of the catalyst **3** following the general procedure described above. The product was obtained exclusively in 62% yield (NMR) after 6 h of reaction.

Characterization Data for (3′-Nitrobenzyl)-3-nitrobenzoate. ^{1}H NMR (500 MHz, $C_6D_5CD_3$): δ 4.78 (s, 2H, -CH_2), 8.58 (s, 1H, Ph), 7.88 (s, 1H, Ph), 7.64 (dd, 2H, Ph), 7.58 (d, J = 6.9 Hz, 1H, Ph), 6.37−6.51 (m, 3H, Ph). ^{13}C NMR (125 MHz, $C_6D_5CD_3$): δ 68.5, 127.3, 129.1, 129.8, 131.4, 131.6, 133.6, 134.5, 136.4, 139.6, 140.2. MS: m/z 302 (M^+), 150 ($ArCO^+$), 136 ($ArCH_2^+$).

Esterification of *o*-Furanaldehyde. The esterification product (2′-furylmethyl)-2-furancarboxylate was obtained by the reaction of 0.98 mmol of *o*-furanaldehyde and 6.5 mg (0.01 mmol) of the catalyst **3** at 60 °C. The progress of the reaction was monitored continuously with the help of ^{1}H NMR. After 48 h, the products were identified by NMR and GC/MS analysis. The ester product was obtained exclusively in 42% yield (NMR) after 48 h of reaction at 60 °C.

Characterization Data for (2′-Furylmethyl)-2-furancarboxylate. ^{1}H NMR (500 MHz, $C_6D_5CD_3$): δ 5.02 (s, 2H, -CH_2), 5.96−6.07 (m, 1H, aromatic), 5.96−6.04 (m, 2H), 6.11−6.15 (m, 1H, aromatic), 6.97−7.08 (dd, 2H, aromatic). ^{13}C NMR (125 MHz, $C_6D_5CD_3$): 58.0, 110.8, 111.2, 111.7, 118.2, 137.5, 142.2, 143.3, 146.3, 153.6. MS: m/z 190 (M^+).

Esterification of Terephthalaldehyde. The esterification product poly[*p*-(carboxymethylene)phenylene] was obtained by the reaction of 0.98 mmol of terephthalaldehyde and 6.5 mg (0.01 mmol) of the catalyst **3** in toluene. The product was precipitated out of the solution,

filtered off, and washed with toluene 3−4 times prior to analysis. The product was obtained in 60% yield (NMR) after 6 h of reaction.

Characterization Data for Polyester of Poly[p-(carboxymethylene)phenylene]. ^{1}H NMR (500 MHz, $C_2D_2Cl_4$): δ 4.63−4.71 (m, 18H, -CH_2), 5.29−5.37 (m, 28H, -CH_2), 7.20−7.46 (m, 52H, Ph), 8.00−8.07 (m, 40H, Ph) 9.92 and 9.95 (s, 2H, -*CHO*). ^{13}C NMR (125 MHz, C_2D_2Cl): δ 64.4, 64.8, 65.7, 66.2, 66.3, 126.4, 127.1, 127.5, 128.0, 128.3, 129.6, 129.8, 129.9.

Cross-Esterification. In a typical experiment, the NMR tube was charged in the glovebox with 5 mg of Cp_2*$ThMe_2$ (0.0092 mmol) and dissolved with benzene-d_6, benzaldehyde (0.095 mL, 0.94 mmol; 0.047 mL, 0.47 mmol), and *p*-tolualdehyde (0.105 mL, 0.94 mmol; 0.052 mL, 0.47 mmol). The reaction was allowed to stand at room temperature for 2 days, and the products were identified by ^{1}H NMR. The ratio between the four products was calculated by integration of the four benzylic signals appearing at δ 5.13 ppm for (4′-methylbenzyl)-4-methylbenzoate (**5**), δ 5.12 ppm and δ 5.11 ppm for **6** and **7**, and δ 5.09 ppm for benzyl benzoate (**4**). MS: *m*/*z* 226 (M^+).

Recycled Experiment. To determine the longevity of the catalyst, typical recycled experiments were carried out with the catalyst **3**. After completion of one batch of dimerization reaction, the NMR tube was dried overnight in a high-vacuum line, and a reddish brown mass was obtained. The tube was then taken inside a glovebox, the reddish brown mass was dissolved in C_6D_6, and a new batch of benzaldehyde (0.098 mmol) was added. The reaction was again monitored by ^{1}H NMR spectroscopy, and the product was isolated as described in the general procedure.

Kinetic Study of the Esterification of Benzaldehyde. In a glovebox, a J. Young NMR tube with a Teflon valve (previously flamed in vacuum) was charged with complex Cp_2*$ThMe_2$ (5−40 mg, 0.0092−0.074 mmol as a solution in benzene-d_6) or $Me_2SiCp''_2ThBu_2$ (1.90 mg, from a 110.5 mM stock solution) and benzaldehyde (0.03− 0.200 mL, 0.295−1.88 mmol). The mixture was then immediately diluted to 400 μL with benzene-d_6/toluene-d_8. The tube was frozen in liquid nitrogen until NMR measurements were initiated. The tube was defrosted and quickly inserted into the NMR probe, which had been maintained at 30 °C, and an initial spectrum was recorded. Data were acquired using eight scans per time interval sequence. The progress of the reaction was monitored by the disappearance of the aldehyde signal around δ 9.56 ppm and the appearance of the proton α to carbonyl around δ 5.06 ppm over three half-lives. The concentration of the coupling product at time *t* was determined from the area of the ^{1}H integrals of the product (α protons to carbonyl group), standardized to the total area of resonances of the aldehyde proton of the starting material and the product.

Influence of the Catalyst Concentration. The influence of catalyst concentration on the reaction rate at a specific temperature was determined by using different catalysts (**1** and **3**) and concentrations (7.37×10^{-3}−2.95×10^{-2}M), while the concentration of the aldehyde (7.37×10^{-1} M) and temperature (30 °C) were kept constant. The rate constant, k_{obs} ($M\ s^{-1}$), was calculated from the pseudo-linear part of the plot of the product concentration vs time. The k_{obs} showed a linear increase with increasing catalyst concentration. Hence, we deduce that the reaction is first-order dependent on the catalyst.

Influence of the Benzaldehyde Concentration. To determine the aldehyde concentration dependence on reaction rate, the reaction was carried out with a varying concentration of benzaldehyde (7.37×10^{-1}−2.45 M), while the catalyst (**1** and **3**), concentration (7.37×10^{-3} M), and temperature (30 °C) were kept constant. The rate constant, k_{obs} ($M\ s^{-1}$), was calculated from the pseudo-linear part of the plot of the product concentration vs time. The plot of k_{obs} against the concentration showed a good linear fit, revealing that the reaction is first-order in aldehyde concentration.

Further, to determine the limiting catalyst:substrate ratio, in a similar way as mentioned above, k_{obs} was determined by increasing the concentration of benzaldehyde up to 5.39 M from 2.45 M while the concentration of the catalyst **3** was kept constant (7.37×10^{-3} M).

Influence of the Temperature. The influence of temperature on the reaction rate was investigated by carrying out the Tishchenko reaction at different temperatures (35, 55, 75, and 95 °C) with constant concentrations of the catalyst (7.37×10^{-3} M) and aldehyde (7.37×10^{-1} M).

A plot of product concentration vs time was made, and from the pseudo-linear part of the plot, the rate constant, k_{obs} ($M\ s^{-1}$), was calculated at each temperature. The energy of activation for the RDS was calculated from the Arrhenius equation ($\ln k = \ln A_0 - E_a/RT$, where *R* is the gas constant, 1.987 cal $mol^{-1}\ K^{-1}$). From the slope of the linear plot of $\ln(k_{obs})$ as a function of $1/T$, the value $-E_a/R$ can be found, and the activation energy for the rate-determining step can be calculated.

The enthalpy of activation ($\Delta H^{\ddagger}$) and entropy of activation ($\Delta S^{\ddagger}$) for the RDS were calculated by using the Eyring equation,

$$k = (\kappa T/h)\, e^{-\Delta H^{\ddagger}/RT}\, e^{\Delta S^{\ddagger}/R} \rightarrow$$

$$\ln(k/T) = \ln(\kappa/h) - \Delta H^{\ddagger}/RT + \Delta S^{\ddagger}/R$$

where κ is the Boltzmann constant, 1.38×10^{-23} J/K, and *h* is Planck's constant, 6.626×10^{-34} J·s.

Therefore, the slope of the plot $\ln(k/T)$ vs $1/T$ represents the value $-\Delta H^{\ddagger}/R$, and the intersection with the *Y*-axis is the sum of $\ln(\kappa/h)$ and $\Delta S^{\ddagger}/R$.

In a similar way, the thermodynamic parameters E_a, $\Delta H^{\ddagger}$, and $\Delta S^{\ddagger}$ were also determined for *para*- and *meta*-substituted chloro- and methylbenzaldehydes.

Kinetic Isotopic Effect. In a typical experiment, a 5 mm NMR tube was charged in a glovebox with **1** (5 mg, 0.0092 mmol as a solution in benzene-d_6), benzaldehyde and α-d-benzaldehyde (0.060 mL, 0.593 mmol). Benzene-d_6 was then added to bring the total volume of the solution to 0.5 mL. The tube was closed, quickly removed from the glovebox, and maintained in liquid nitrogen until NMR measurements were initiated. The sample was quickly warmed and inserted into the probe, and an initial spectrum was recorded. Data were acquired using eight scans per time interval sequence. The progress of the reaction was monitored by the disappearance of the aromatic signal of the reactant at δ 7.8 ppm and the appearance of the product at δ 8.1 ppm over three half-lives. The concentration of the coupling product at time *t* was determined from the area of the ^{1}H integrals of the product standardized to the total area of resonances of the aldehyde proton of the starting material and the product. The value k_H/k_D was calculated from the pseudo-linear part of each reaction.

Computational Details. The equilibrium molecular structures as well as transition-state geometries were optimized using the hybrid density functional B3LYP.[34] The Stuttgart basis set in combination with the 60-core−electron relativistic effective core potential (SDD)[35] was used for thorium; 6-31G*[36] basis sets were used for carbon, hydrogen, and oxygen. The effects of polarization and diffusion functions were tested on C, H, and O atoms in single-point calculations and found to be negligible (see Supporting Information). Spin−orbit interactions have not been considered explicitly. After each successful optimization, frequency calculations were performed to confirm that the structures were minima or saddle points. All transition structures contained exactly one imaginary frequency and were linked to reactant, products, or intermediates using intrinsic reaction coordinate (IRC)[37] calculations. All thermodynamic data were calculated at the standard state (298.15 K and 1 atm). The solvent effect was also tested by the PCM (SCRF) model[38] using toluene as solvent and the effect was found to be negligible (see Supporting Information), which is quite expected due to the low dielectric constant of toluene. All calculations were carried out with the Gaussian03 suite of codes.[39] All Mülliken, NBO electron densities, and bonding analyses were done using the NBO technique.[40]

The NBO analysis describes donor−acceptor interactions according to a second-order perturbation theory.

■ ASSOCIATED CONTENT

Supporting Information. Typical NMR spectra showing concomitant formation of dimeric ester product from benzaldehyde, computational details of all structures (Cartesian coordinates, Gibbs free energies), and complete ref 39. This material is available free of charge via the Internet at http://pubs.acs.org.

■ AUTHOR INFORMATION

Corresponding Author
chmoris@tx.technion.ac.il

■ ACKNOWLEDGMENT

This research was supported by the Israel Science Foundation Administered by the Israel Academy of Science and Humanities, under Contract No. 518/09. M.S. thanks the Lady Davis Trust for a postdoctoral Fellowship. We are also indebted to the Australian Research Council and the Australian Partnership for Advanced Computing (APAC) for all computing facilities. Author M.S. is also thankful to Prof. Peter Boyd (at the University of Auckland) for valuable suggestions and discussion.

■ REFERENCES

(1) (a) Ulrich, D.; Jankowski, H. *Chem. Tech. (Leipzig)* **1988,** *40,* 393–397.(b) Weissermel, K.; Arpe., H.-J. *Industrial Organic Chemistry, Completely Revised,* 4th ed.; Wiley-VCH: Weinheim, 2003.

(2) (a) Claisen, L. *Ber. Dtsch. Chem. Ges.* **1887,** *20,* 655–657. (b) Tischtschenko, W. *Chem. Zentralbl.* **1906,** *771,* 1309. (c) Tischtschenko, W. *J. Russ. Phys. Chem.* **1906,** *38,* 355–418.

(3) (a) Hawkins, E. G. E.; Long, D. J. G.; Major, F. W. *J. Chem. Soc.* **1955,** 1462–1468.(b) Frostick, F. R.; Phillips, B. (Union Carbide &Carbon Corp.). U.S. Patent A-2716123, 1953; *Chem. Abstr.* **1953,** *50,* 7852f.(c) Child, W. C.; Adkins, H. *J. Am. Chem. Soc.* **1925,** *47,* 798–807. (d) Villani, F. J.; Nord, F. F. *J. Am. Chem. Soc.* **1947,** *69,* 2605–2607. (e) Lin, I.; Day, A. R. *J. Am. Chem. Soc.* **1952,** *74,* 5133–5135. (f) Seki, T.; Nakajo, T.; Onaka, M. *Chem. Lett.* **2006,** *35,* 824–829.

(4) Stapp, P. R. *J. Org. Chem.* **1973,** *38,* 1433–1434.

(5) (a) Yamashita, M.; Watanabe, Y.; Mitsudo, T.-a.; Takegami, Y. *Bull. Chem. Soc. Jpn.* **1976,** *49,* 3597–3600. (b) Yamashita, M.; Ohishi, T. *Appl. Organomet. Chem.* **1993,** *7,* 357–361.

(6) Morita, K.; Nishiyama, Y.; Ishii, Y. *Organometallics* **1993,** *12,* 3748–3752.

(7) (a) Horino, H.; Ito, T.; Yamamoto, A. *Chem. Lett.* **1978,** 17–20. (b) Ito, T.; Horino, H.; Koshiro, Y.; Yamamoto, A. *Bull. Chem. Soc. Jpn.* **1982,** *55,* 504–512.

(8) Bergens, S. H.; Fairlie, D. P.; Bosnich, B. *Organometallics* **1990,** *9,* 566–571.

(9) (a) Onozawa, S.-y.; Sakakura, T.; Tanaka, M.; Shiro, M. *Tetrahedron* **1996,** *52,* 4291–4302. (b) Burgstein, M. R.; Berberich, H.; Roesky, P. W. *Chem.—Eur. J.* **2001,** *7,* 3078–3085. (c) Zuyls, A.; Roesky, P. W.; Deacon, G. B.; Konstas, K.; Junk, P. C. *Eur. J. Org. Chem.* **2008,** 693–697. (d) Berberich, H.; Roesky, P. W. *Angew. Chem., Int. Ed.* **1998,** *37,* 1569–1571.

(10) Barrio, P.; Esteruelas, M. A.; Onate, E. *Organometallics* **2004,** *23,* 1340–1348.

(11) Suzuki, T.; Yamada, T.; Matsuo, T.; Watanabe, K.; Katoh, T. *Synlett* **2005,** 1450–1452.

(12) (a) Luo, Y.; Selvam, P.; Koyama, M.; Kubo, M.; Miyamoto, A. *Chem. Lett.* **2004,** *33,* 780–785. (b) Hong, S.; Marks, T. J. *Acc. Chem. Res.* **2004,** *37,* 673–686. (c) Brennan, J. G.; Sella, A. *J. Organomet. Chem.* **2002,** *30,* 91–115. (d) Hou, Z.; Wakatsuki, Y. *Coord. Chem. Rev.* **2002,** *231,* 1–22. (e) Edelmann, F. T.; Freckmann, D. M. M.; Schumann, H. *Chem. Rev.* **2002,** *102,* 1851–1896. (f) Molander, G. A.; Dowdy, E. D. *Top. Organomet. Chem.* **1999,** *2,* 119–154. (g) Anwander, R.; Herrmann, W. A. *Top. Curr. Chem.* **1996,** *179,* 1–32. (h) Edelmann, F. T. *Top. Curr. Chem.* **1996,** *179,* 247–276. (i) Schumann, H.; Meese-Marktscheffel, J. A.; Esser, L. *Chem. Rev.* **1995,** *95,* 865–986. (j) Schaverien, C. J. *Adv. Organomet. Chem.* **1994,** *36,* 283–362. (k) Evans, W. J. *Adv. Organomet. Chem.* **1985,** *24,* 131–177.(l) Schumann, H. In *Fundamental and Technological Aspects of Organo-f-Element Chemistry*; Marks, T. J., Fragala, I., Eds.; D. Reidel: Dordrecht, Holland, 1985; Chapter 1.(m) Barnea, E.; Eisen, M. S. *Coord. Chem. Rev.* **2006,** *250,* 855–899. (n) Evans, W. J. *J. Organomet. Chem.* **2002,** *652,* 61–68. (o) Leal, J. P.; Calhorda, M. J. *Chemtracts* **2000,** *13,* 804–809. (p) Ephritikhine, M. *New J. Chem.* **1992,** *16,* 451–469. (q) Ephritikhine, M. *Chem. Rev.* **1997,** *97,* 2193–2242. (r) Berthet, J. C.; Ephritikhine, M. *Coord. Chem. Rev.* **1998,** *178−180,* 83–116. (s) Edelmann, F. T.; Lorenz, V. *Coord. Chem. Rev.* **2000,** *209,* 99–160. (t) Edelmann, F. T.; Gun'ko, Y. K. *Coord. Chem. Rev.* **1997,** *165,* 163–237. (u) Blake, P. C.; Edelman, M. A.; Hitchcock, P. B.; Hu, J.; Lappert, M. F.; Tian, S.; Muller, G.; Atwood, J. L.; Zhang, H. *J. Organomet. Chem.* **1998,** *551,* 261–270. (v) Hitchcock, P. B.; Hu, J.; Lappert, M. F.; Tian, S. *J. Organomet. Chem.* **1997,** *536/537,* 473–480. (w) Edelman, M. A.; Hitchcock, P. B.; Hu, J.; Lappert, M. F. *New J. Chem.* **1995,** *19,* 481–489.

(13) (a) Fendrick, C. M.; Schertz, L. D.; Day, V. W.; Marks, T. J. *Organometallics* **1988,** *7,* 1828–1838. (b) Bruno, J. W.; Stecher, H. A.; Morss, L. R.; Sonnenberger, D. C.; Marks, T. J. *J. Am. Chem. Soc.* **1986,** *108,* 7275–7280. (c) Smith, G. M.; Carpenter, J. D.; Marks, T. J. *J. Am. Chem. Soc.* **1986,** *108,* 6805–6807. (d) Broach, R. W.; Schultz, A. J.; Williams, J. M.; Brown, G. M.; Manriquez, J. M.; Fagan, P. J.; Marks, T. J. *Science (Washington, D.C.)* **1979,** *203,* 172–174. (e) Jones, S. B.; Fagan, P. J.; Manriquez, J. M.; Maatta, E. A.; Seyam, A. M.; Marks, T. J. *J. Am. Chem. Soc.* **1981,** *103,* 6650–6667. (f) Lin, Z.; Marks, T. J. *J. Am. Chem. Soc.* **1990,** *112,* 5515–5525. (g) Straub, T.; Haskel, A.; Eisen, M. S. *J. Am. Chem. Soc.* **1995,** *117,* 6364–6365. (h) Haskel, A.; Straub, T.; Dash, A. K.; Eisen, M. S. *J. Am. Chem. Soc.* **1999,** *121,* 3014–3024. (i) Wang, J.; Dash, A. K.; Kapon, M.; Berthet, J.-C.; Ephritikhine, M.; Eisen, M. S. *Chem.—Eur. J.* **2002,** *8,* 5384–5396. (j) Wang, J. Q.; Dash, A. K.; Berthet, J. C.; Ephritikhine, M.; Eisen, M. S. *Organometallics* **1999,** *18,* 2407–2409. (k) Dash, A. K.; Wang, J. X.; Berthet, J. C.; Ephritikhine, M.; Eisen, M. S. *J. Organomet. Chem.* **2000,** *604,* 83–98. (l) Chen, Y.-X.; Metz, M. V.; Li, L.; Stern, C. L.; Marks, T. J. *J. Am. Chem. Soc.* **1998,** *120,* 6287–6305. (m) Jia, L.; Yang, X.; Stern, C. L.; Marks, T. J. *Organometallics* **1997,** *16,* 842–857. (n) Haskel, A.; Straub, T.; Eisen, M. S. *Organometallics* **1996,** *15,* 3773–3775. (o) Straub, T.; Frank, W.; Reiss, G. J.; Eisen, M. S. *J. Chem. Soc., Dalton Trans.* **1996,** 2541–2546. (p) Eisen, M. S.; Straub, T.; Haskel, A. *J. Alloys Compd.* **1998,** *271−273,* 116–122. (q) Straub, T.; Haskel, A.; Neyroud, T. G.; Kapon, M.; Botoshansky, M.; Eisen, M. S. *Organometallics* **2001,** *20,* 5017–5035. (r) Eisen, M. S. *Chem. Org. Silicon Compd.* **1998,** *2,* 2037–2128. (s) Eisen, M. S. *Rev. Inorg. Chem.* **1997,** *17,* 25–53. (t) Wang, J. X.; Dash, A. K.; Berthet, J. C.; Ephritikhine, M.; Eisen, M. S. *J. Organomet. Chem.* **2000,** *610,* 49–57.

(14) Haskel, A.; Wang, J. Q.; Straub, T.; Neyroud, T. G.; Eisen, M. S. *J. Am. Chem. Soc.* **1999,** *121,* 3025–3034.

(15) Dash, A. K.; Wang, J. Q.; Eisen, M. S. *Organometallics* **1999,** *18,* 4724–4741.

(16) Barnea, E.; Andrea, T.; Kapon, M.; Berthet, J.-C.; Ephritikhine, M.; Eisen, M, S. *J. Am. Chem. Soc.* **2004,** *126,* 10860–10861.

(17) (a) Wang, J.; Gurevich, Y.; Botoshansky, M.; Eisen, M. S. *J. Am. Chem. Soc.* **2006,** *128,* 9350–9351. (b) Andrea, T.; Eisen, M. S. *Chem. Soc. Rev.* **2008,** *37,* 550–567.

(18) Stern, D.; Sabat, M.; Marks, T. J. *J. Am. Chem. Soc.* **1990,** *112,* 9558–9575.

(19) Marks, T. J.; Streitwiser, J. A. In *The Chemistry of the Actinide Elements*,2nd ed.; Katz, J. J., Seaborg, G. T., Morss, L. R., Eds.; Chapman and Hall: London, 1986; Vol. 2.

(20) (a) Bursten, B. E.; Strittmatter, R. J. *Angew. Chem.* **1991,** *103,* 1085–1103; *Angew. Chem., Int. Ed. Engl.* **1991,** *1030,* 1069–1085. (b) Tatsumi, K.; Nakamura, A. *J. Am. Chem. Soc.* **1987,** *109,* 3195–3206.

(21) (a) Jeske, G.; Lauke, H.; Mauermann, H.; Schumann, H.; Marks, T. J. *J. Am. Chem. Soc.* **1985,** *107,* 8111–8118. (b) Jeske, G.; Schock, L. E.; Swepston, P. N.; Schumann, H.; Marks, T. J. *J. Am. Chem. Soc.* **1985,** *107,* 8103–8110. (c) Fendrick, C. M.; Mintz, E. A.; Schertz, L. D.; Marks, T. J. *Organometallics* **1984,** *3,* 819–821. (d) Schnabel, R. C.; Scott, B. L.; Smith, W. H.; Burns, C. J. *J. Organomet. Chem.* **1999,** *591,* 14–23. (e) Dash, A. K.; Gourevich, I.; Wang, J. Q.; Wang, J.; Kapon, M.; Eisen, M. S. *Organometallics* **2001,** *20,* 5084–5104.

(22) (a) Gagne, M. R.; Marks, T. J. *J. Am. Chem. Soc.* **1989,** *111,* 4108–4109. (b) Giardello, M. A.; Conticello, V. P.; Brard, L.; Gagne, M. R.; Marks, T. J. *J. Am. Chem. Soc.* **1994,** *116,* 10241–10254.

(23) Lin, Z.; Marks, T. J. *J. Am. Chem. Soc.* **1987,** *109,* 7979–7985.

(24) (a) Barnea, E.; Moradove, D.; Berthet, J.-C.; Ephritikhine, M.; Eisen, M. S. *Organometallics* **2006,** *25,* 320–322. (b) Herrmann, W. A.; Anwander, R.; Kleine, M.; Oefele, K.; Riede, J.; Scherer, W. *Chem. Ber.* **1992,** *125,* 2391–2397. (c) Berg, D. J.; Burns, C. J.; Andersen, R. A.; Zalkin, A. *Organometallics* **1989,** *8,* 1865–1870. (d) Schumann, H.; Palamidis, E.; Loebel, J. *J. Organomet. Chem.* **1990,** *384,* C49–C52. (e) Beeckman, W.; Goffart, J.; Rebizant, J.; Spirlet, M. R. *J. Organomet. Chem.* **1986,** *307,* 23–37.

(25) (a) Evans, W. J.; Grate, J. W.; Bloom, I.; Hunter, W. E.; Atwood, J. L. *J. Am. Chem. Soc.* **1985,** *107,* 405–409. (b) Eisen, M. S.; Marks, T. J. *J. Am. Chem. Soc.* **1992,** *114,* 10358–10368. (c) Eisen, M. S.; Marks, T. J. *Organometallics* **1992,** *11,* 3939–3941. (d) Eisen, M. S.; Marks, T. J. *J. Mol. Catal.* **1994,** *86,* 23–50.

(26) Wang, J.; Gurevich, Y.; Botoshansky, M.; Eisen, M. S. *Organometallics* **2008,** *27,* 4494–4504.

(27) Andrea, T.; Barnea, E.; Eisen, M. S. *J. Am. Chem. Soc.* **2008,** *130,* 2454–2455.

(28) (a) Cramer, C. J.; Truhlar, D. G. *Phys. Chem. Chem. Phys.* **2009,** *11,* 10757–10816. (b) Brookes, N. J.; Ariafard, A.; Stranger, R.; Yates, B. F. *J. Am. Chem. Soc.* **2009,** *131,* 5800–5808. (c) Brookes, N. J.; Ariafard, A.; Stranger, R.; Yates, B. F. *Dalton Trans.* **2009,** 9266–9272. (d) Ariafard, A.; Brookes, N. J.; Stranger, R.; Yates, B. F. *J. Am. Chem. Soc.* **2008,** *130,* 11928–11938. (e) Ariafard, A.; Yates, B. F. *J. Organomet. Chem.* **2009,** *694,* 2075–2084.

(29) (a) Clark, D. L.; Gordon, J. C.; Hay, P. J.; Poli, R. *Organometallics* **2005,** *24,* 5747–5758. (b) Schelter, E. J.; Yang, P.; Scott, B. L.; Da Re, R. E.; Jantunen, K. C.; Martin, R. L.; Hay, P. J.; Morris, D. E.; Kiplinger, J. L. *J. Am. Chem. Soc.* **2007,** *129,* 5139–5152. (c) Shamov, G. A.; Schreckenbach, G.; Martin, R. L.; Hay, P. J. *Inorg. Chem.* **2008,** *47,* 1465–1475. (d) Graves, C. R.; Yang, P.; Kozimor, S. A.; Vaughn, A. E.; Clark, D. L.; Conradson, S. D.; Schelter, E. J.; Scott, B. L.; Thompson, J. D.; Hay, P. J.; Morris, D. E.; Kiplinger, J. L. *J. Am. Chem. Soc.* **2008,** *130,* 5272–5285. (e) Yang, P.; Warnke, I.; Martin, R. L.; Hay, P. J. *Organometallics* **2008,** *27,* 1384–1392. (f) Cantat, T.; Graves, C. R.; Jantunen, K. C.; Burns, C. J.; Scott, B. L.; Schelter, E. J.; Morris, D. E.; Hay, P. J.; Kiplinger, J. L. *J. Am. Chem. Soc.* **2008,** *130,* 17537–17551. (g) Austin, J. P.; Sundararajan, M.; Vincent, M. A.; Hillier, I. H. *Dalton Trans.* **2009,** 5902–5909. (h) Gaunt, A. J.; Reilly, S. D.; Enriquez, A. E.; Scott, B. L.; Ibers, J. A.; Sekar, P.; Ingram, K. I. M.; Kaltsoyannis, N.; Neu, M. P. *Inorg. Chem.* **2008,** *47,* 29–41. (i) Schreckenbach, G.; Shamov, G. A. *Acc. Chem. Res.* **2010,** *43,* 19–29. (j) Balcells, D.; Clot, E.; Eisenstein, O. *Chem. Rev.* **2010,** *110,* 749–823.

(30) O'Hagan, D.; Goss, R. J. M.; Meddour, A.; Courtieu, J. *J. Am. Chem. Soc.* **2003,** *125,* 379–387.

(31) (a) Manriquez, J. M.; Fagan, P. J.; Marks, T. J.; Day, C. S.; Day, V. W. *J. Am. Chem. Soc.* **1978,** *100,* 7112–7114. (b) Fagan, P. J.; Manriquez, J. M.; Marks, T. J.; Day, V. W.; Vollmer, S. H.; Day, C. S. *J. Am. Chem. Soc.* **1980,** *102,* 5393–5396.

(32) (a) Simoes, J. A. M.; Beauchamp, J. L. *Chem. Rev.* **1990,** *90,* 629–688. (b) McMillen, D. F.; Golden, D. M. *Annu. Rev. Phys. Chem.* **1982,** *33,* 493–532.

(33) (a) Manriquez, J. M.; Fagan, P. J.; Marks, T. J. *J. Am. Chem. Soc.* **1978,** *100,* 3939–3941. (b) Stubbert, B. D.; Stern, C. L.; Marks, T. J. *Organometallics* **2003,** *22,* 4836–4838.

(34) (a) Becke, A. D. *Phys. Rev. A: Gen. Phys.* **1988,** *38,* 3098–3100. (b) Becke, A. D. *J. Chem. Phys.* **1993,** *98,* 5648–5652. (c) Lee, C.; Yang, W.; Parr, R. G. *Phys. Rev. B: Condens. Matter* **1988,** *37,* 785–789. (d) Stephens, P. J.; Devlin, F. J.; Chabalowski, C. F.; Frisch, M. J. *J. Phys. Chem.* **1994,** *98,* 11623–11627.

(35) (a) Kuechle, W.; Dolg, M.; Stoll, H.; Preuss, H. *J. Chem. Phys.* **1994,** *100,* 7535–7542. (b) Dolg, M.; Stoll, H.; Preuss, H.; Pitzer, R. M. *J. Phys. Chem.* **1993,** *97,* 5852–5859.

(36) Hariharan, P. C.; Pople, J. A. *Theor. Chim. Acta* **1973,** *28,* 213–222.

(37) Gonzalez, C.; Schlegel, H. B. *J. Phys. Chem.* **1990,** *94,* 5523–5527.

(38) (a) Miertus, S.; Scrocco, E.; Tomasi, J. *Chem. Phys.* **1981,** *55,* 117–129. (b) Miertus, S.; Tomasi, J. *Chem. Phys.* **1982,** *65,* 239–245. (c) Cramer, C. J.; Truhlar, D. G. *Chem. Rev.* **1999,** *99,* 2161–2200. (d) Tomasi, J.; Mennucci, B.; Cammi, R. *Chem. Rev.* **2005,** *105,* 2999–3093.

(39) Frisch, M. J. et al. *Gaussian 03,* Revision E.01; Gaussian Inc.: Wallingford, CT, 2004.

(40) Reed, A. E.; Curtiss, L. A.; Weinhold, F. *Chem. Rev.* **1988,** *88,* 899–926.